Interior Alaska Amphibolite Mineral Compositions: A Key to Distinguishing Metamorphic Assemblage

Rainer J. Newberry and Jamshid A. Moshrefzadeh

Preliminary Interpretive Report 2026-2

Fine-grained biotite-hornblende-plagioclase amphibolite with alternating impure marble layers about 5-10 cm thick. Mount Harper project field station 22ADW036. https://maps.dggs.alaska.gov/photodb/detail/50782

Preliminary Interpretive Reports present emergent interpretations of geologic mapping or analytical investigation. These publications are reviewed for clarity and consistency and receive limited peer review.

State of Alaska
Department of Natural Resource
Division of Geological & Geophysical Surveys

STATE OF ALASKA
Mike Dunleavy, Governor

DEPARTMENT OF NATURAL RESOURCES
John Crowther, Commissioner

DIVISION OF GEOLOGICAL & GEOPHYSICAL SURVEYS
Erin Campbell, State Geologist & Director

Publications produced by the Division of Geological & Geophysical Surveys are available to download from the DGGS website (dggs.alaska.gov). Publications on hard-copy or digital media can be examined or purchased in the Fairbanks office:

Alaska Division of Geological & Geophysical Surveys (DGGS)
3354 College Road | Fairbanks, Alaska 99709-3707
Phone: 907.451.5010 | Fax 907.451.5050
dggspubs@alaska.gov | dggs.alaska.gov

DGGS publications are also available at:

Alaska State Library, Historical
Collections & Talking Book Center
395 Whittier Street
Juneau, Alaska 99801

Alaska Resource Library and
Information Services (ARLIS)
3150 C Street, Suite 100
Anchorage, Alaska 99503

Suggested citation:
Newberry, R.J., and Moshrefzadeh, J.A., 2026, Interior Alaska amphibolite mineral compositions: A key to distinguishing metamorphic assemblage: Alaska Division of Geological & Geophysical Surveys Preliminary Interpretive Report 2026-2, 33 p. https://doi.org/10.14509/32081

INTERIOR ALASKA AMPHIBOLITE MINERAL COMPOSITIONS: A KEY TO DISTINGUISHING METAMORPHIC ASSEMBLAGE

Rainer J. Newberry and Jamshid A. Moshrefzadeh

ABSTRACT

Metamorphic rocks in eastern Interior Alaska have historically been grouped into various packages and, more recently, assemblages. These assemblages are commonly distinguished from one another by $^{40}Ar/^{39}Ar$ age dating, a relatively expensive and time-consuming technique. In some cases, there is a clear difference in metamorphic grade between assemblages, but in others, there is none. Three different amphibolite-facies units (Fortymile River, Lake George, and Fairbanks-Chena assemblages) have been identified (Dusel-Bacon and others, 2006) that include similar constituent lithologies with no obvious hand-specimen distinctions. Contact and retrograde metamorphism have locally overprinted the rocks, further complicating the situation. We present electron microprobe mineral-compositional data for 79 metamafic rocks collected between 1981 and 2024 (primarily 2021–2024) to distinguish assemblages based on amphibole and plagioclase compositions. Most analyses presented here were performed using standard-energy-dispersive spectrometry (EDS), except for samples collected in 2024, which were analyzed using more accurate wavelength-dispersive spectrometry (WDS). Several samples were analyzed by both techniques and show broadly comparable results. Amphibole compositions appear to show better discrimination as plagioclase is susceptible to later recrystallization from both higher-temperature (contact-type) metamorphism and lower-temperature (retrograde) metamorphism. This study partly confirms the assignments shown in Dusel-Bacon (2006) but shows evidence that the Fairbanks-Chena assemblage is more widespread than previously indicated.

In addition to the discussion presented here, we provide data tables for the set, which includes sample identifiers, geographic locations and description, petrographic locations, mineral phases, oxide weight percentages, and calculated cation proportions for amphibole and plagioclase populations. These data and accompanying discussion are released as a DGGS Preliminary Interpretive Report, and all publication components are available from the DGGS website at https://doi.org/10.14509/32081.

INTRODUCTION

Interior Alaska consists mostly of metamorphic and plutonic rocks. The former have been divided into several different assemblages based on a variety of criteria, including constituent lithologies, metamorphic facies, thermochronology/geochronology, and spatial association (fig. 1). These assemblages, as defined by Dusel-Bacon and others (2006), include Klondike, Fortymile River, Ladue, Chicken, Butte, Blackshell, Fairbanks–Chena, and Lake George assemblages, along with the Seventymile terrane. Greenschist facies metamafic rocks contain (by definition) actinolite and albite (plus additional minerals), whereas amphibolite facies metamafic rocks typically contain hornblende (in the broad sense), plagioclase, and additional minerals characteristic of amphibolite facies.

[1]Alaska Division of Geological & Geophysical Surveys, 3354 College Road, Fairbanks, AK 99709

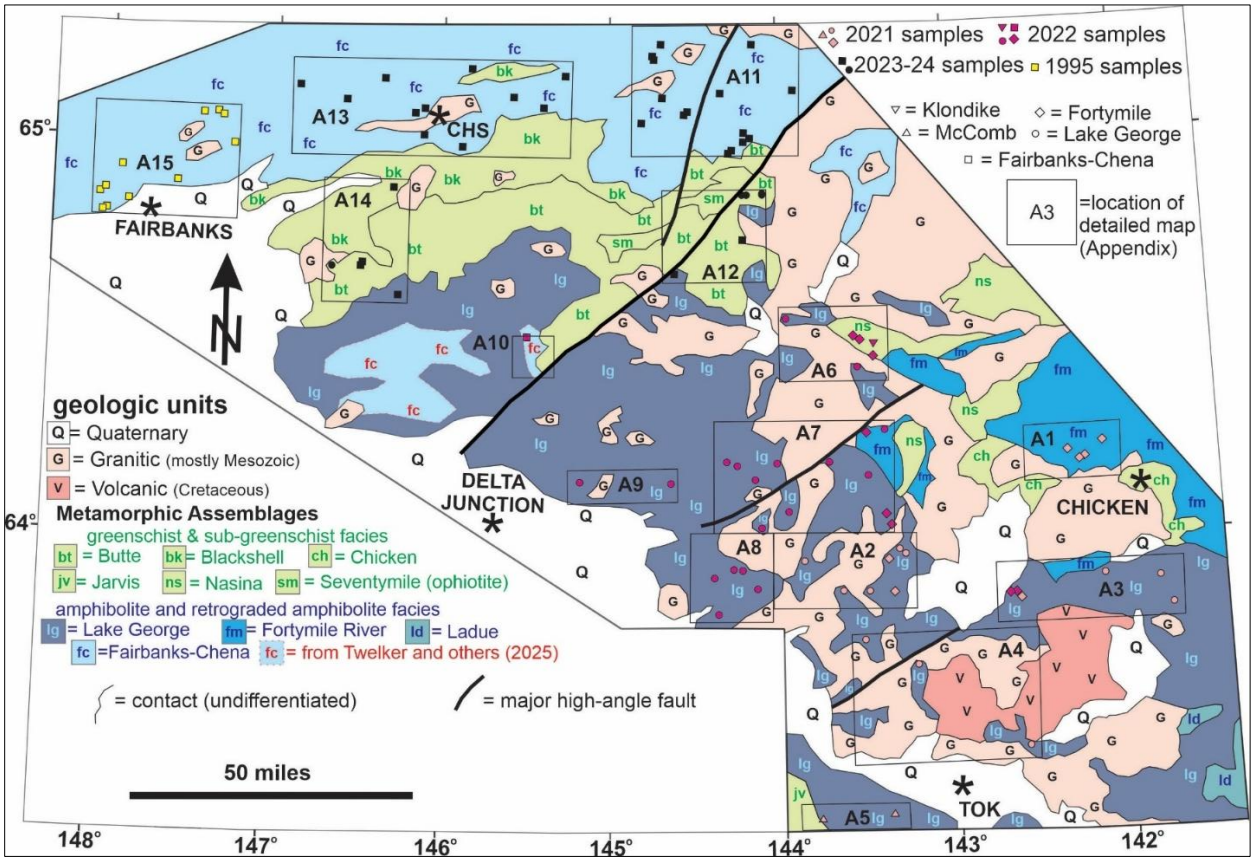

Figure 1. Generalized geology (mostly modified from Dusel-Bacon and others, 2006) and location map for samples used in this study. CHS = Chena Hot Springs. Black boxes indicate the location of the detailed maps (in the Appendix) discussed in this study.

Metamafic rocks are commonly employed to distinguish different packages of metamorphic rocks. Dusel-Bacon and others (2006) attempted to use trace-element characteristics to distinguish metamafic rocks from different assemblages, with mixed results, most notably in distinguishing the Seventymile terrane from the other assemblages. Newberry and Twelker (2021) began using plagioclase and amphibole compositions to distinguish units in the eastern Tanacross Quadrangle.

Geologic mapping by DGGS in 2021–2024 required distinguishing between Klondike, Fortymile River, Lake George, and Fairbanks-Chena assemblages; the last three are amphibolite facies and contain similar lithologies and textures. Lake George assemblage rocks are thought to structurally underlie Fortymile River assemblage rocks, but the contact is a low-angle structure that is commonly offset by later high-angle faults. Consequently, establishing which assemblage is present in each area can be challenging. Dusel-Bacon and others (2006) mapped the Lake George and Fairbanks-Chena assemblages as separated by a belt of greenschist-facies rocks (the Blackshell, Butte, and Seventymile units). The Fairbanks-Chena assemblage lies to the north of this greenschist belt, while the Lake George assemblage lies to the south (fig. 1). However, Twelker and others (2025) have identified an area of Fairbanks-Chena assemblage rocks south of the greenschist

facies belt in the northern Richardson Mining district. This raises the possibility that Fairbanks-Chena assemblage may occur south of the greenschist facies belt elsewhere in Interior Alaska, conflicting with the long-standing description by Dusel-Bacon and others (2006).

Thin-section petrography showed that approximately half of the Lake George amphibolite samples commonly contain garnet and lack primary epidote-clinozoisite. Diopside was identified (and confirmed by electron microprobe) in about 10 percent of the samples, and biotite is a common accessory mineral. Conversely, all Fortymile River and Fairbanks-Chena samples lack diopside, and most lack garnet but contain primary-appearing epidote-clinozoisite. Fortymile River amphibolite from the northernmost part of the 2021 mapping area contains garnet, and about one-third of the Fairbanks area amphibolites contain garnet and epidote. In summary, Lake George amphibolites experienced amphibolite facies conditions, whereas Fortymile River and Fairbanks-Chena amphibolites generally experienced lower-temperature "epidote-amphibolite" conditions. However, due to the variable presence of garnet in all three and the difficulty in distinguishing primary from secondary epidote-clinozoisite, thin-section petrography was not sufficient to reliably distinguish between the three types.

Major element plots for Lake George, Fortymile River, and Fairbanks-Chena amphibolites show considerable variation, but no systematic differences (fig. 2). Figure 2A illustrates SiO_2 vs. CaO for samples from Lake George, Fortymile River, and Fairbanks-Chena assemblages, and includes linear regression lines for the three assemblages. The average values shown in the Na_2O vs. K_2O plot (fig. 2B) are nearly identical. The lack of significant differences in major oxide composition is shown in table 1. Standard deviations for each oxide are typically two to three times larger than the compositional differences between assemblages. In other words, there are no systematic differences in major element composition. Thus systematic differences in plagioclase compositions (Na-Ca) between different types (for example, as shown in Newberry and Twelker, 2021) cannot be due to differences in rock composition.

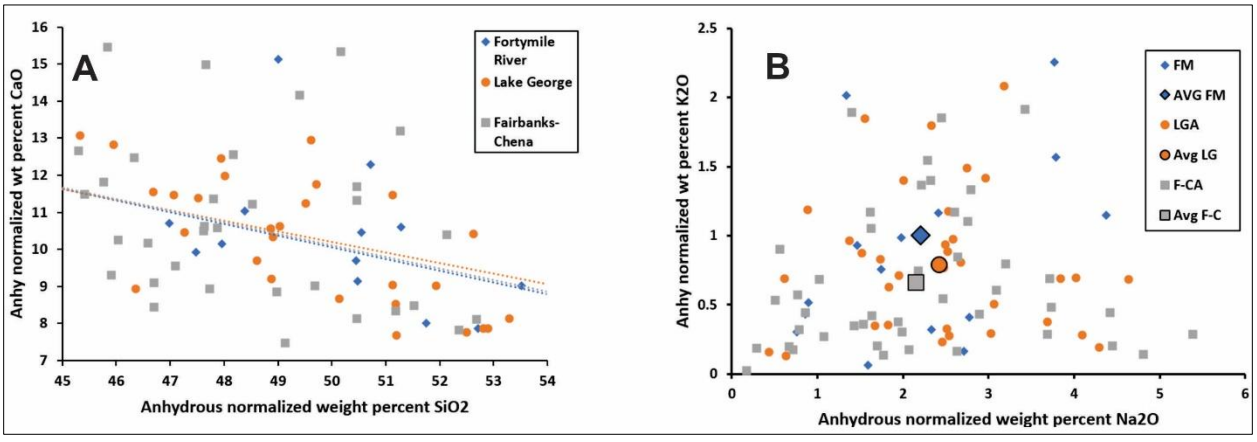

Figure 2. Compositional plots for amphibolite samples from three Interior Alaska metamorphic assemblages. **A.** SiO_2 vs. CaO; colored lines are best-fit linear regression lines, color-coded to the three data sets. **B.** Na_2O vs. K_2O; data from Wypych and others (2018, 2022A, 2022B, 2023) and Buchanan and others (2025).

Table 1. Average and standard deviation for major element compositions of Fairbanks-Chena, Lake George, and Fortymile River assemblage amphibolites (stdev = standard deviation, n = number of analyses). FC = Fairbanks–Chena, LG = Lake George, FR = Fortymile River

Oxide	FC (n=44) Mean	FC (n=44) StDev	LG (n=34) Mean	LG (n=34) StDev	FR (n=16) Mean	FR (n=16) StDev
SiO_2	47.4	3.5	48.4	3.5	49.4	2.8
TiO_2	2.2	1.1	1.9	1.1	1.3	0.7
Al_2O_3	13.3	2.8	14.3	2.2	15.8	1.8
Fe_2O_3	12.5	1.8	12.3	2.4	11.1	3.1
MnO	0.18	0.05	0.2	0.05	0.2	0.06
MgO	8.5	2.9	7.3	2.3	7	1.8
CaO	10.5	2.4	10.3	1.8	9.7	1.9
Na_2O	2.1	1.2	2.4	1	2.2	1.1
K_2O	0.64	0.5	0.77	0.5	1	0.8
P_2O_5	0.36	0.3	0.26	0.2	0.28	0.3

Specific Geologic Issues Addressed

Detailed maps showing amphibolite samples selected for microprobe analyses across the Yukon Tanana Uplands region are included in the appendix to this report. Individual map locations are shown in figure 1.

The 2021 samples were collected during fieldwork in support of the Northwest Tanacross and Taylor Mountain geologic mapping projects (Naibert and others, 2024; Wypych and others, 2024). Regional geologic maps (e.g., Dusel-Bacon and others, 2006) show a single, continuous fault between the Lake George and Fortymile River assemblages, but subsequent mapping (e.g., Twelker and others, 2021) demonstrates that the contact is considerably displaced, both vertically and horizontally, by younger steeply dipping faults. The analyses presented in this study aim to distinguish the Fortymile River and Lake George assemblage samples.

A Fortymile River amphibolite in the far northeastern part of the Taylor Mountain map area (21RN568) is complicated by an obscure contact between more typical epidote amphibolite and rarer amphibolite facies rocks (fig. A1). This difference is partly reflected in the mineral composition, as discussed further in this report. Complex faulting occurs to the southwest, juxtaposing different amphibolite units (fig. A2). In contrast, simpler relationships occur farther south (figs. A3 and A4). Wypych and others (2024) mapped a narrow strip in the eastern Alaska Range in part to determine if the so-called McComb subterrane of Nokleberg and others (1992) is Lake George assemblage and to define the contact between it and the Jarvis assemblage (Naibert and others, 2024; fig. A5).

Fieldwork in 2022 was conducted in a geologically diverse area stretching from the Mount Harper map area in the Eagle Quadrangle to the Lake George area in the Mt Hayes Quadrangle, and west to the Richardson Mining District in the southern Big Delta Quadrangle. Microprobe analyses in this report aimed to distinguish between Fortymile River, Klondike, and Lake George

assemblages in the Eagle Quadrangle, and to test the presence of the Fairbanks-Chena assemblage south of the greenschist belt (fig. 1), as identified from limited amphibolite data by Twelker and others (2025b). Detailed maps (Appendix) are presented from northeast to southwest and show the complexity of the Lake George–Fortymile River relationship in the northeast (figs. A6 and A7) and the predominance of Lake George assemblage to the west (figs. A8 and A9). The farthest-west amphibolite examined in this group (fig. A10) exhibits Fairbanks-Chena characteristics.

Fieldwork in 2023 and 2024 was primarily conducted in the greenschist belt (fig. 1) or to the north, presumably in the Fairbanks-Chena assemblage rocks. Due to wildfires in summer 2023, as well as access issues, there was considerable overlap between the areas mapped in 2023 and 2024 (figs. A11-A14). DGGS geologists made multiple traverses south of, or within, amphibolite-facies rocks within the greenschist belt. Consequently, our investigations were designed to test: (a) the hypothesis that Fairbanks-Chena amphibolites could be successfully distinguished from Lake George amphibolites, and (b) whether more occurrences of Fairbanks-Chena rocks south of the greenschist belt could be identified. Because 2024 samples were analyzed differently from 2021–2023 samples (EDS vs. WDS, respectively), the former are considered separately.

In the farthest-east region of the study area, north of the greenschist belt, samples were expected to exhibit Fairbanks-Chena characteristics (fig. A11). Samples from farther to the southwest are at the southern end of the greenschist belt and were expected to show Lake George characteristics (fig. A12). The entire Chena Hot Springs area lies north of the main greenschist belt and is therefore expected to contain Fairbanks-Chena characteristics (fig. A13). Several samples were collected near the Chena Hot Spring batholith to examine recrystallization-related effects (fig. A13). In contrast, the Granite Tors–Eielson area is mostly within an area of amphibolite-facies rocks complexly intermixed with greenschist-facies rocks (fig. A14). Most of our samples were taken from amphibolites occurring in areas previously mapped as greenschist facies. One sample (23ET235) was from south of the greenschist facies belt (fig. A14) and thus was expected to be part of the Lake George assemblage (Dusel-Bacon and others, 2006).

We unearthed WDS analyses for amphibolite samples collected in 1995 and earlier as part of past DGGS mapping efforts (Newberry, unpub., 1995; Newberry and others, 1996). Previous mapping (Robinson and others, 1990) divided Fairbanks metamorphic rocks into three groups: (a) rocks equivalent to the Blackshell unit, (b) the Chena River units (amphibolite facies), and (c) most of the area as Fairbanks schist units (greenschist facies). However, Newberry and others (1996) suggested that the Fairbanks schist and Chena River units were both amphibolite facies and indistinguishable. Amphibolites from the two units were therefore analyzed to show that the amphiboles from the two units were hornblende, and the feldspars were plagioclase. Samples were collected from both units (fig. A15). Although the analyses were not published, Joy and others (1996) reported data on minerals from schistose rocks that showed indistinguishable pressure-temperature conditions.

METHODS

Analytical Methods

While mapping in 2021–2024, geologists selected samples for preparation as polished thin sections (fig. 1). We examined all the thin sections produced (typically 200–300 per field season) and selected metamafic samples that showed minimal weathering or retrograde alteration. For example, thin sections with significant alteration of hornblende to actinolite and/or chlorite, or alteration of plagioclase to white mica, calcite, and/or chlorite were rejected. At least four sites on each thin section containing amphibole and plagioclase were randomly selected for standard-modified energy-dispersive spectroscopy (EDS) analyses using the electron probe microanalyzer (EPMA). Typically, at least three grains each of amphibole and plagioclase were analyzed at least three times at each thin-section site. Additional analyses were conducted to confirm the presence of specific minerals (e.g., clinopyroxene). All analyses were performed using the JEOL JXA-8530 Field Emission EPMA at the University of Alaska Fairbanks Advanced Instrumentation Laboratory (UAF-AIL) under standard conditions for standards and unknowns (as described in Newberry and Twelker, 2021).

We also analyzed 2024 samples using wavelength-dispersive spectrometry (WDS; reported in Moshrefzadeh and Newberry, 2025) to obtain more accurate results and to verify standard-modified EDS analyses of the 2024 samples (and those from previous years). Due to analytical variability, three or more analyses from a single grain were averaged. To compare analyses using the two methods, figure 3 shows the average mole percent anorthite ($CaAl_2Si_2O_8$) component in plagioclase from 23 samples analyzed by both methods. The ‘error’ bars are 1 standard deviation and indicate the considerable range in compositions seen in many samples. Most average analyses fall on or very close to the 1:1 line; even those with large compositional variations fall close to the line.

We also discovered previously unpublished hornblende and plagioclase analyses made using the Cameca SX-50 microprobe at UAF-AIL by WDS techniques (as described in Joy and others, 1996), (Newberry, unpub., 1995). These were also checked against standard-modified EDS analyses completed in January 2025.

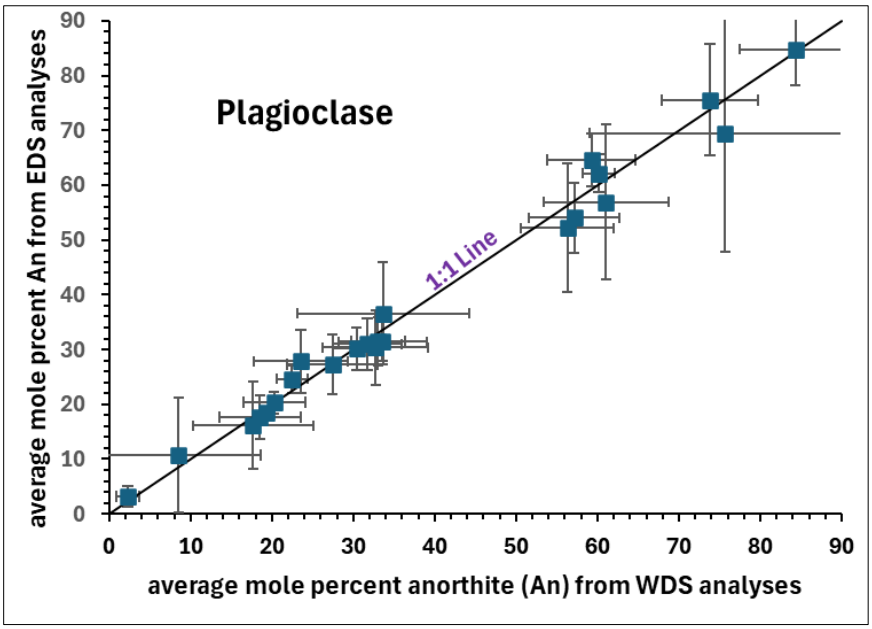

Figure 3. Comparison of average plagioclase compositions using WDS versus standard-modified EDS analyses for 23 samples analyzed 2024-2025 in 2024–2025. 'Error bars' are 1 standard deviation and represent the range of compositions in a given sample, not the analytical errors. Most analyses plot close to the 1:1 line; deviations are due to major compositional variations in some samples.

Mineral Calculations

Amphiboles can be represented by the general formula $A_{0\text{-}1}B_2M_5T_8O_{22}(OH)_2$, where the A site is variably filled and contains Na + K (sodium + potassium); the B site contains all the Ca (calcium) and enough Na (sodium) to fill the site; the M site contains the octahedrally coordinated ions (Mg, Fe, Mn, Ti, and Al not in the T site), and the T site contains ions in tetrahedral coordination (all the Si and enough Al to fill the site). Because hydrogen cannot be analyzed by electron microprobe, the formula is recast as A0-1B2M5T8O23+(H2O) for microprobe analyses; that is, atomic formulas are calculated for 23 oxygens, and the numbers are calculated per formula unit (pfu).

Unlike some silicates (e.g., olivine), the iron in amphibole occurs as both Fe2+ and Fe3+, which the EPMA cannot distinguish. In addition, the sum of all cations except Ca, Na, and K should be 13 (5+8) pfu (the variably filled A site causes the latter three to sum to anywhere between 2 and 3 pfu). The cation calculations depend on the relative amounts of FeO and Fe_2O_3 in a mineral because Fe_2O_3 contains 1.5 oxygens per Fe, whereas FeO contains 1 oxygen per Fe. The mass ratio of Fe_2O_3/2FeO is 1.1113 due to the additional oxygen in Fe2O3. Thus, a standard approach to calculating the relative amounts of Fe^{2+} and Fe^{3+} in amphibole is to assume that all iron is FeO (Rock and Leake, 1984). Generally, doing so will yield atomic Fe+Mg+Mn+Ti+Al+Si pfu > 13. Increasing the ratio of Fe_2O_3/FeO (from zero) causes atomic Fe+Mg+Mn+Ti+Al+Si (pfu) to decrease due to the factors described above. The ratio is gradually increased until the sum exactly equals 13. This procedure yields an improved cation distribution pfu and provides a measure of Fe^{3+}. Applying this technique to the 2021–2024 analyses generally yielded an Fe^{2+}/total iron atomic ratio of 0.7-0.95, which is considered normal based on traditional wet chemical analyses of mineral separates (Deer and others, 1997). Analyses that required considerably more Fe^{3+} (about 5 percent of the total) were rejected as unreliable.

RESULTS

Our approach in presenting the data is both chronological (starting with 2021 samples) and geographic (from east to west). Fortymile River units are largely located in the northeast region of the study area, Lake George units in the southwest, and Chena-Fairbanks units in the northwest (fig. 1), but local structural complications make the pattern (as shown on the detailed maps) considerably more complicated.

2021 Investigations

Some Fortymile River amphiboles contain more Si (pfu) and Na + K (A site) than Lake George amphiboles (fig. 4), as previously noted by Newberry and Twelker (2021). However, several of the Fortymile River amphiboles plot with less Na + K (A site) than those from Lake George. A plot of weight percent TiO_2 vs. K_2O in amphibole (fig. 5) shows that many of the Lake George amphiboles plot exclusively in a high TiO_2-K_2O field, and some Fortymile River amphiboles plot exclusively in a low TiO_2-K_2O field.

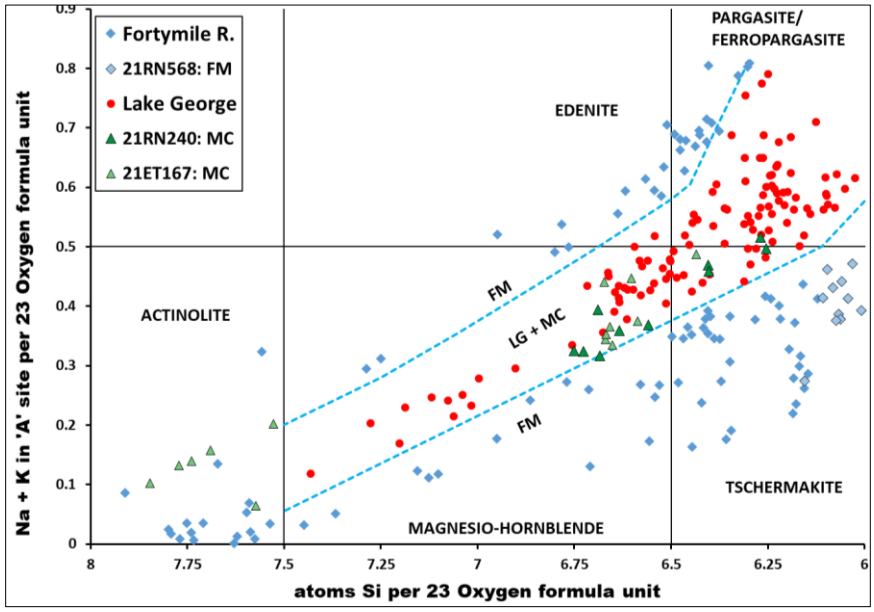

Figure 4. Atoms Si vs. Na + K (A site) for amphiboles from 2021 (and two 2022) amphibolites. Dashed blue line boundaries are empirical, taken from Newberry and Twelker (2021) and this study. Black lines separate different amphibole minerals, modified from Leake and others (1997). FM = Fortymile River; LG = Lake George; MC = McComb.

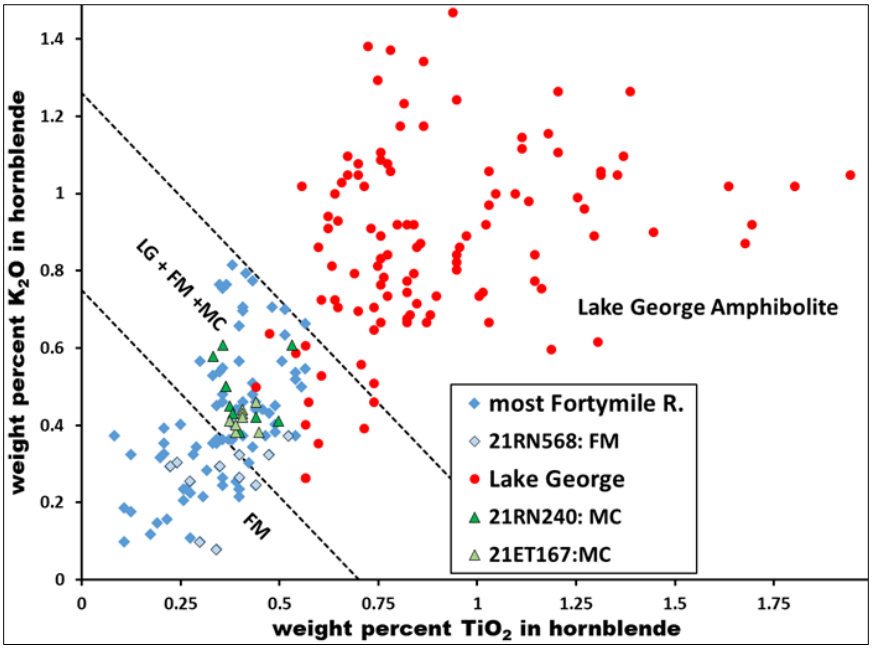

Figure 5. Weight percent TiO2 vs. K2O in 2021 amphibolite hornblende. Dashed black lines are empirical and separate three groups: (a) only Lake George, (b) Lake George, Fortymile River, and McComb, (c) only Fortymile River. FM = Fortymile River; LG = Lake George; MC = McComb.

Plagioclase composition discrimination is more complicated than for amphiboles (fig.6). Almost all 2021 Fortymile River amphibolites contain epidote, and almost all 2021 Lake George amphibolites contain garnet, diopside, and/or biotite. All but one Fortymile River sample contains plagioclase with less than 36 mole percent anorthite (An_{36}; dashed vertical line in fig. 6), whereas all Lake George samples contain a range of plagioclase compositions that include values greater than An_{36}. However, many of the samples display retrograde overprints with significant amounts of secondary albite. Sample 21RN568, from the far northern map area (fig. A1), is the sole example of Fortymile River amphibolite with relatively high-Ca plagioclase (fig. 6); it also lacks epidote and contains significant garnet (9 percent).

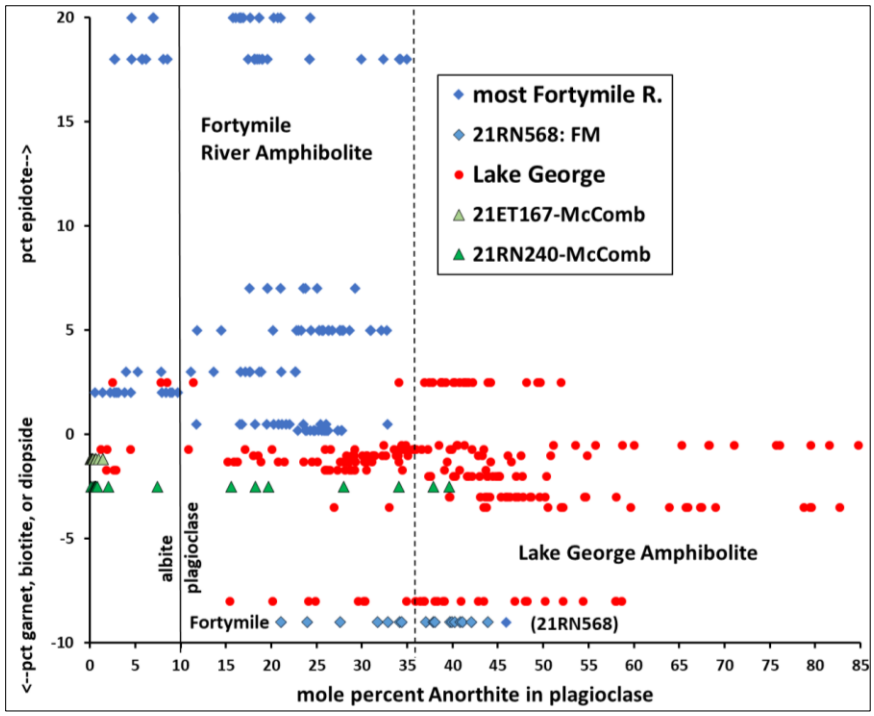

Figure 6. Mole percent anorthite vs. accessory mineralogy for 2021 (and two 2022) amphibolite samples. Pct =percent

The two McComb samples have mineral compositions that generally support a Lake George assignment; the amphiboles plot with those of Lake George samples (figs. 4 and 5). Plagioclase compositions are less straightforward, as both samples contain significant albite overprints. Sample 21RN240 contains a range of compositions up to An_{39}; sample 21ET167 is more altered and contains only albite (fig. 6).

2022 Investigations

Amphiboles from Lake George amphibolite samples mostly fall into the Lake George field (as defined by 2021 samples; fig. 4); there is some overlap with Fortymile River amphiboles in the high-Si part of the pargasite field (fig. 7). On the TiO_2 vs. K_2O diagram (fig. 8), most (three-quarters) of the Lake George amphiboles plot in the high TiO_2-K_2O field of "only Lake George," as defined by 2021 samples (fig. 5). Fortymile River samples mostly fall in the region above Lake George samples (fig. 7): however, three plot in the region below Lake George, similar to 2021 samples (fig. 4).

One sample (22RN477) is from a body mapped as Fairbanks-Chena (fig. A10; Twelker and others, 2025a); this sample also plots below Lake George (fig. 7), while most analyses plot in the "not Lake George" field on the TiO2 vs. K2O diagram (fig. 8). Sample 22ET093 (identified in the field as an amphibolite surrounded by lower grade rocks) actually contains actinolite as the sole amphibole accompanied by albite, clinozoisite, and chlorite. It is a greenschist-facies metamafic rock, consistent with the surrounding rocks (Klondike schist).

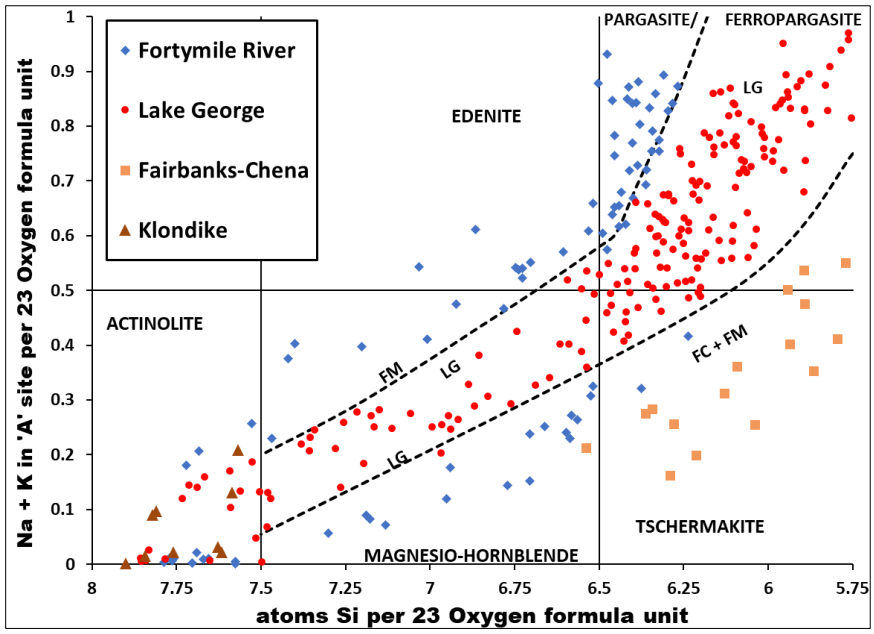

Figure 7. Atoms Si vs. Na + K (A site) for amphiboles from 2022 amphibolites. Dashed black line boundaries are empirical (see fig. 4). Solid black lines separate different amphibole minerals, from Leake and others (1997). FM= Fortymile River, LG=Lake George, FC= Fairbanks-Chena.

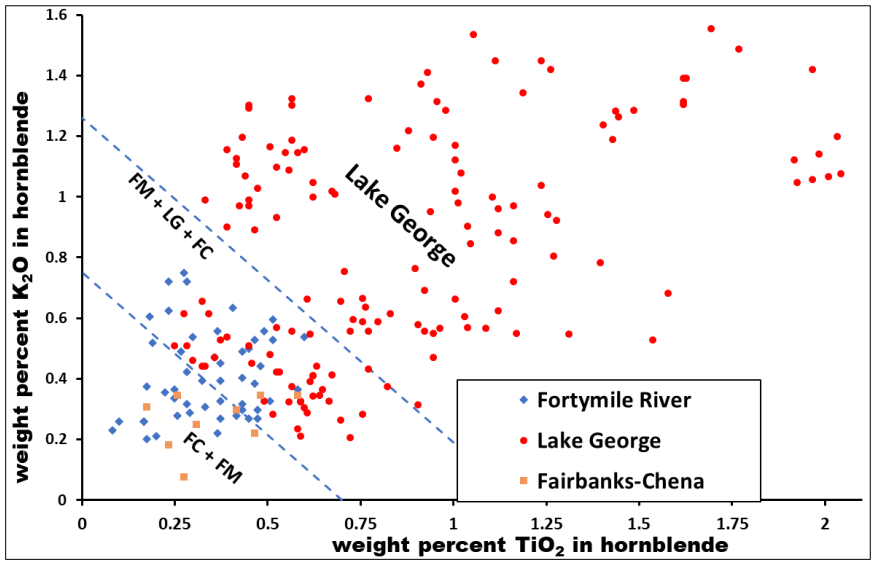

Figure 8. Weight percent TiO2 vs. K2O in hornblende for 2022 samples. Dashed blue lines are empirical and separate three groups: (a) only Lake George; (b) Lake George + Fortymile River + Fairbanks-Chena; and (c) only Fortymile River + Fairbanks-Chena.

Plagioclase compositions from the 2022 samples are mostly straightforward (fig. 9). Fortymile River amphibolite samples yield relatively low-Ca plagioclase (less than An_{35}), and almost all Lake George samples yield at least some plagioclase compositions greater than An_{40}. Lake George sample 22TJN101 lacks garnet, contains five percent epidote, and only yielded a few analyses greater than An_{35} (fig. 9). However, much of the epidote appears secondary and occasionally appears with albite, which are indications of retrograde recrystallization. We suspect that more Ca-rich plagioclase was replaced by albite + epidote during the retrograde event

Sample 22RN477, which plots with non-Lake George amphiboles, contains very calcic plagioclase (fig. 9). This sample is from an area characterized by low-pressure recrystallization in the Fairbanks-Chena rocks, resulting in sillimanite formation in schist (Twelker and others, 2025). Reversely zoned garnet (Mn increases and Mg decreases toward the margin) in the amphibolite

sample is consistent with this. We therefore infer that the highly calcic plagioclase in the sample is due to low-pressure recrystallization.

Sample 22ET093 from greenschist facies Klondike schist contains actinolite (fig. 7), epidote, and sodic albite ($An_{0.8\text{-}1.4}$; fig. 9)

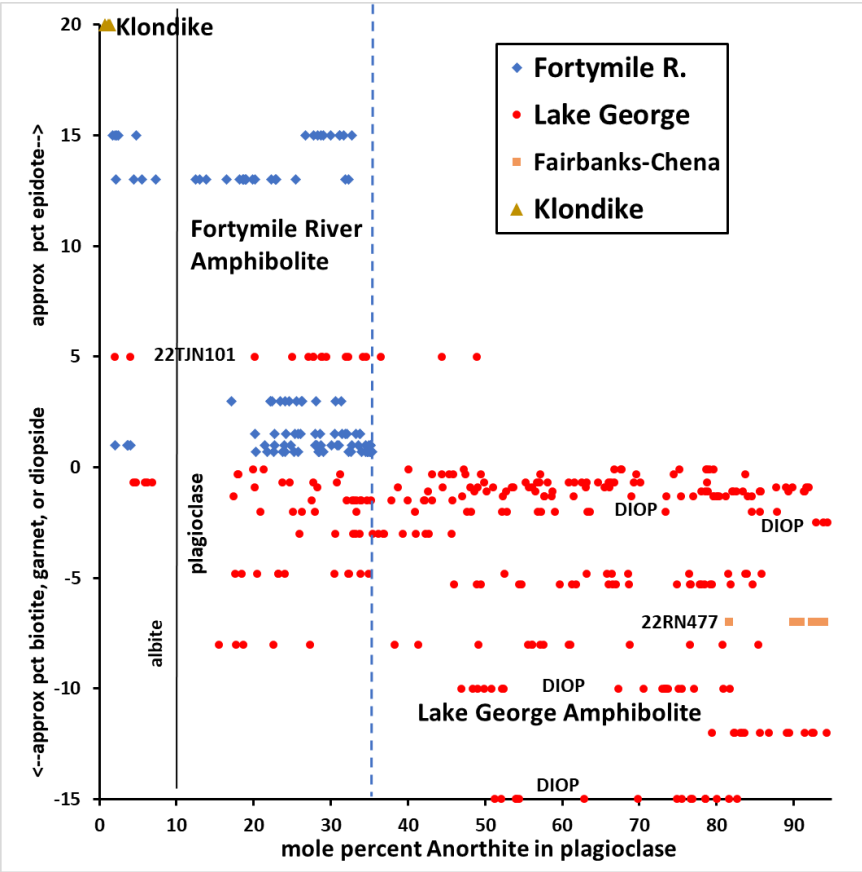

Figure 9. Mole percent anorthite vs. accessory mineralogy for 2022 amphibolite samples and one mafic greenschist. DIOP = diopside, pct = percent

2023 Investigations

All but one of the 2023 samples contain amphiboles with compositions that mostly plot outside the Lake George fields (figs. 10 and 11). The separation is not clean, however, and indicates that the Lake George/Fairbanks-Chena boundary is an empirical one. Two of the samples plot in the field above Lake George on the Si vs. Na + K (A site) diagram, similar to many Fortymile River samples (figs. 4 and 7). Sample 23RN605, the easternmost 2023 sample (fig. A14), plots mostly in the Lake George field on Si vs. Na + K (fig. 10) and in the "permissibly" Lake George field on TiO_2 vs. K_2O (fig. 11). Nearby samples 23Z456 and 23Z458 (fig. A14) mostly plot below Lake George on Si vs. Na + K (A site)—the former entirely and the latter mostly in the "not Lake George" field on TiO_2 vs. K_2O (fig. 11). Only one amphibolite sample from south of the greenschist belt was analyzed in 2023 (23AW123; figs. 1 and A12); this sample (black stars) has apparent Fairbanks-Chena characteristics and plots far from Lake George fields (figs. 10 and 11).

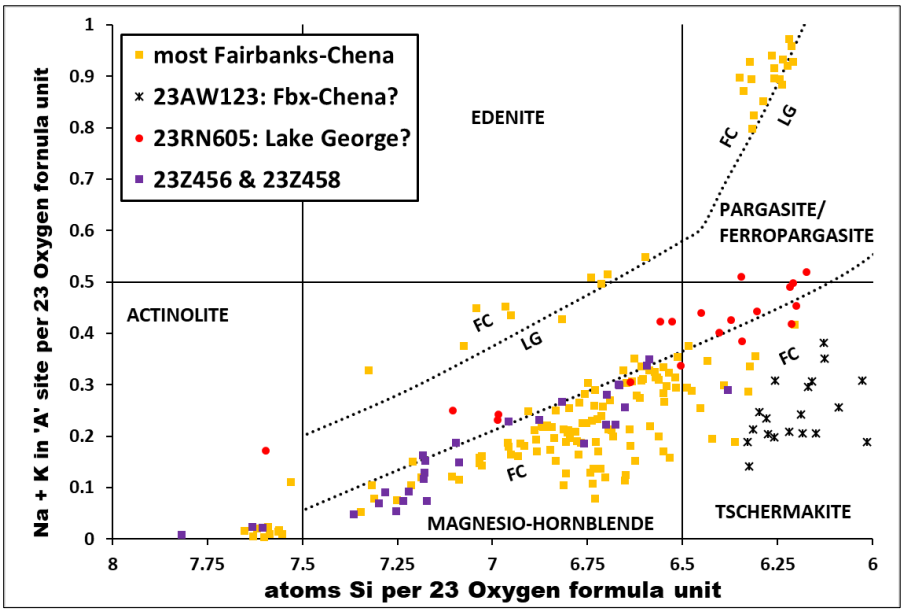

Figure 10. Atoms of Si vs. Na + K (A site) for amphiboles from 2023 amphibolites. FC = Fairbanks-Chena, LG = Lake George. Dashed black line boundaries are empirical. Solid black lines separate different amphibole minerals, from Leake and others (1997).

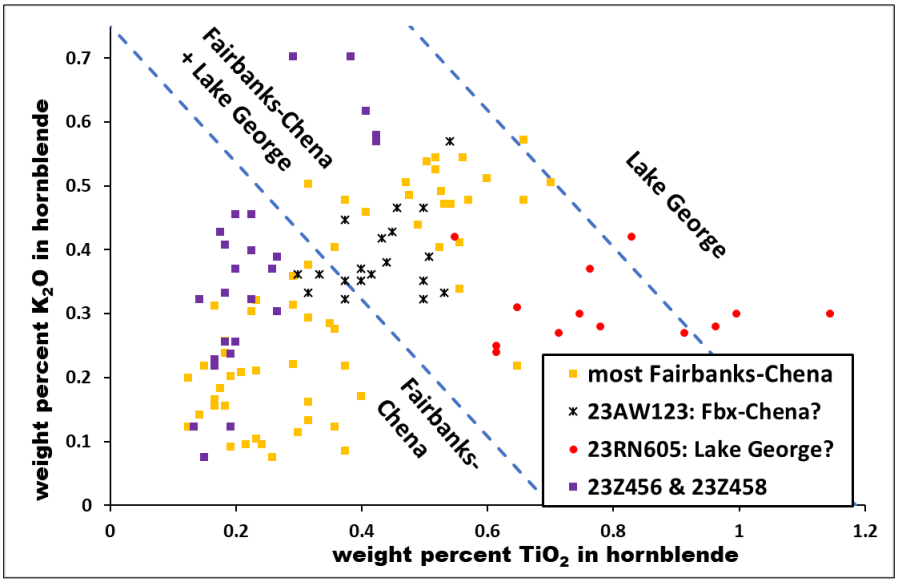

Figure 11. Weight percent TiO2 vs. K2O in hornblende for 2023 samples. Dashed blue lines are empirical and separate three groups: (a) only Lake George; (b) Lake George + Fairbanks-Chena; and (c) only Fairbanks-Chena.

Plagioclase compositions from 2023 samples (fig. 12) were more straightforward than amphibole, in part because all samples were collected more than 2 km from granitic bodies and show little evidence of recrystallization. All samples contained epidote, mostly with textures suggesting the mineral is not part of a greenschist overprint. This is consistent with the relatively uncommon late albite observed in the rocks (fig. 12). All samples yielded plagioclase with less than An_{41} component except 23RN605. Plagioclase ($An_{37–58}$) from that sample is similar to that from 2021 and 2022 Lake George amphibolite samples (figs. 6 and 9). This sample lacks garnet, but that is not uncommon for Lake George amphibolite. The small amount of epidote in the sample is of ambiguous origin.

Plagioclase from sample 23AW123 (south of the greenschist belt, fig. A12) is slightly more calcic (An_{16-41}; fig. 12) than typical for Fortymile River plagioclase (figs. 6 and 9), but Fortymile River and Fairbanks-Chena amphibolites do not need to have the same plagioclase compositions. Samples 23Z456 and 23Z458 (collected from an ambiguous location, but near Lake George type amphibolite; fig. A14) have unambiguous compositions that are not Lake George plagioclase (An_{4-24} and An_{3-25}, respectively; fig. 12).

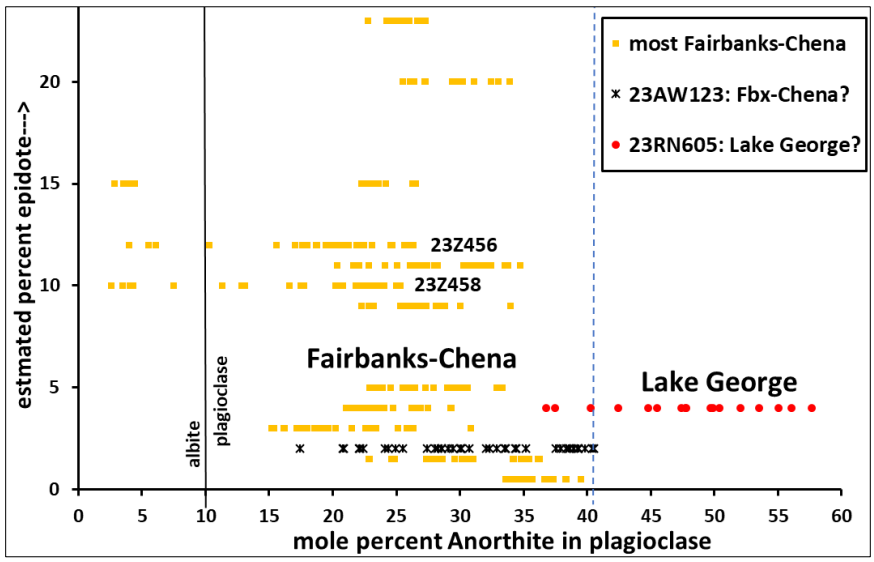

Figure 12. Mole percent anorthite vs. percent epidote for 2023 amphibolite samples.

2024 Investigations

We analyzed the 2024 samples and one 2023 sample (23ET235) using WDS on the EPMA at UAF-AIL to achieve more accurate, quantitative analyses of mineral phases (Moshrefzadeh and Newberry, 2025). In addition to identifying and distinguishing samples, we compared previous standard-modified EDS results with the more accurate WDS analyses (fig. 3). We also chose several samples to look for the anomalous calcic plagioclase associated with recrystallization first identified in sample 22RN477 (fig. 9).

Amphibole compositions identified by WDS separate into distinct Lake George and Fairbanks-Chena groups (figs. 13 and 14). This is particularly true for TiO_2 vs. K_2O (fig. 14). Three of the four (clearly) Lake George samples are from an area just south of the greenschist belt (fig. A12); however, note that two other samples from the same general area (23AW123 and 24Z060; fig. A12) have Fairbanks-Chena characteristics (figs. 10, 11, 13 and 14). The other (clearly) Lake George sample is 24RN515, found near another Lake George sample in the Eielson area (fig. A14). Conversely, sample 23ET235 from south of the greenschist belt (fig. A14) exhibits Fairbanks-Chena characteristics (fig. 13 and 14).

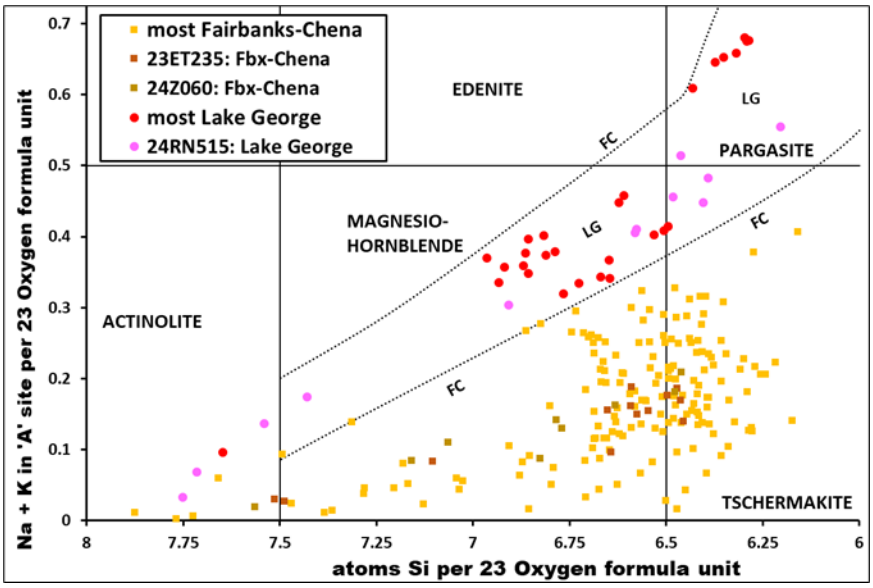

Figure 13. Atoms of Si vs. Na + K (A site) for amphiboles analyzed in 2024. Dashed black line boundaries are empirical. LG = Lake George, FC = Fairbanks-Chena. Solid black lines separate different amphibole minerals, from Leake and others (1997).

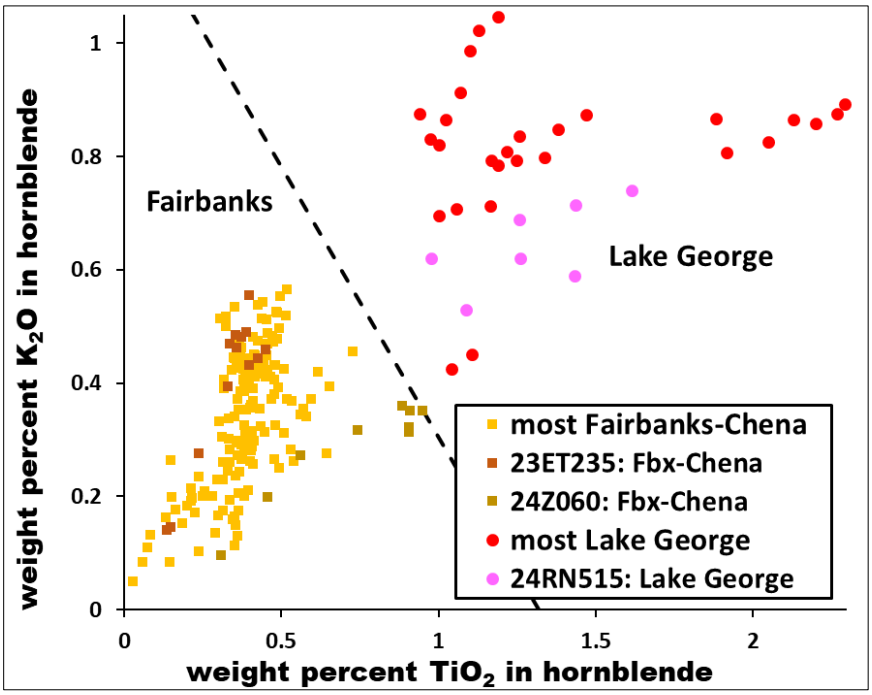

Figure 14. Weight percent TiO_2 vs. K_2O in hornblende for 2024 WDS analyses. The dashed black line is empirical and separates Lake George from Fairbanks-Chena samples.

Plagioclase compositions show several complications. All 2024 Lake George samples yielded plagioclase of at least $An_{42,}$ and most Fairbank-Chena samples yielded lower-Ca plagioclase (less than An_{41}; fig. 15). However, three of the Fairbanks-Chena samples contained high- to very-high-Ca plagioclase (up to $An_{81–94}$; fig. 15) despite having amphiboles with Fairbanks-Chena compositions (figs. 13 and 14). The most obvious case is sample 24RN391, located approximately 100 meters south of the contact with the Chena Hot Springs batholith (fig. A13). This sample contains relict $An_{23–36}$ plagioclase grains within a matrix of $An_{73–85}$ plagioclase (fig. 15). This sample (three kilometers north of the greenschist belt) must be from the Fairbanks-Chena assemblage; the plagioclase composition has been reset, and the amphiboles have not appreciably changed (figs. 13

and 14). Although the plagioclase has been more intensely recrystallized, we interpret sample 24JWB158 to be similar (150 m south of a large granite body; fig. A11). A large granite body is located 2.5 km north of sample 24RN259, but at an unknown depth below it (fig. A11). We interpret the An_{68} plagioclase as altered relict and the $An_{83–94}$ plagioclase (intergrown with quartz) as contact metamorphic. This sample also contains appreciable (15 percent) primary epidote and lacks garnet, both of which support a Fairbanks-Chena assignment.

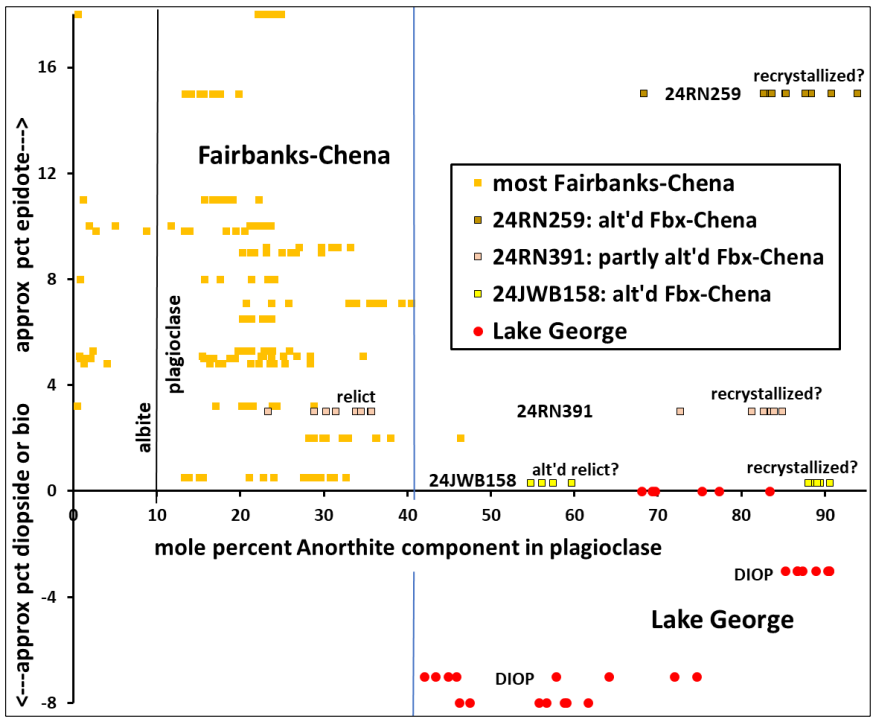

Figure 15. Mole percent anorthite vs. accessory mineralogy for amphibolite samples analyzed in 2024. Diop = diopside; bio = biotite, alt'd = altered, pct = percent

2025 and 1996 Investigations of 1995 Samples

We incorporated old WDS (1996) analyses of 1995 Fairbanks project samples and the polished thin sections from that project. Several of these samples were re-analyzed in 2024 by standard-modified EDS techniques at UAF-AIL.

Fairbanks-area amphibolites are unusual for the Fairbanks-Chena assemblage, as many samples contain garnet, though it is not readily apparent in hand specimens. The amphibole compositions, however, clearly fall outside of the Lake George field in terms of cation assignments (fig. 16), and none plot in the "only Lake George field" on the TiO_2 vs. K_2O diagram (fig. 17). Two-thirds of the analyses plot as tschermakite; hornblende (*sensu stricto*) is less common than observed in other Fairbanks-Chena amphiboles (figs. 10 and 13).

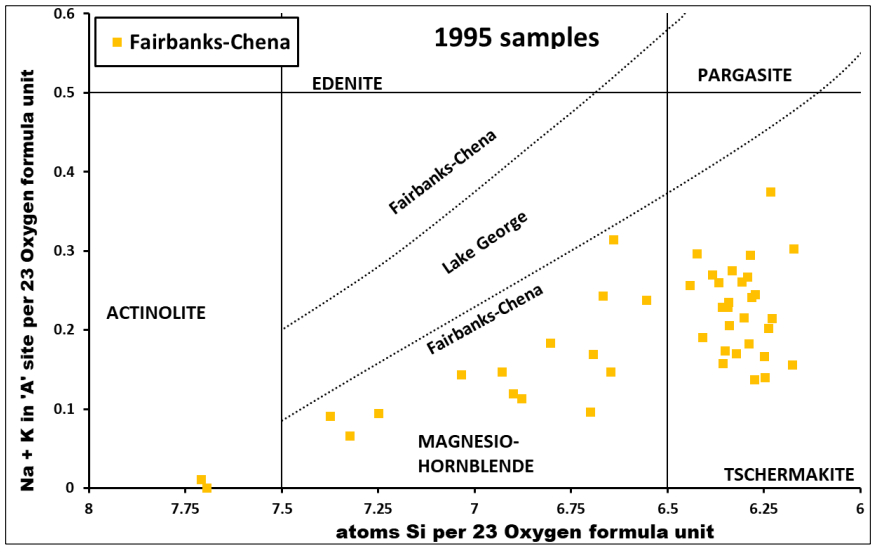

Figure 16. Atoms of Si versus Na + K (A site) for Fairbanks area amphibolite amphiboles analyzed in 1996 and 2025. Dashed black line boundaries are empirical. Solid black lines separate different amphibole minerals, from Leake and others (1997).

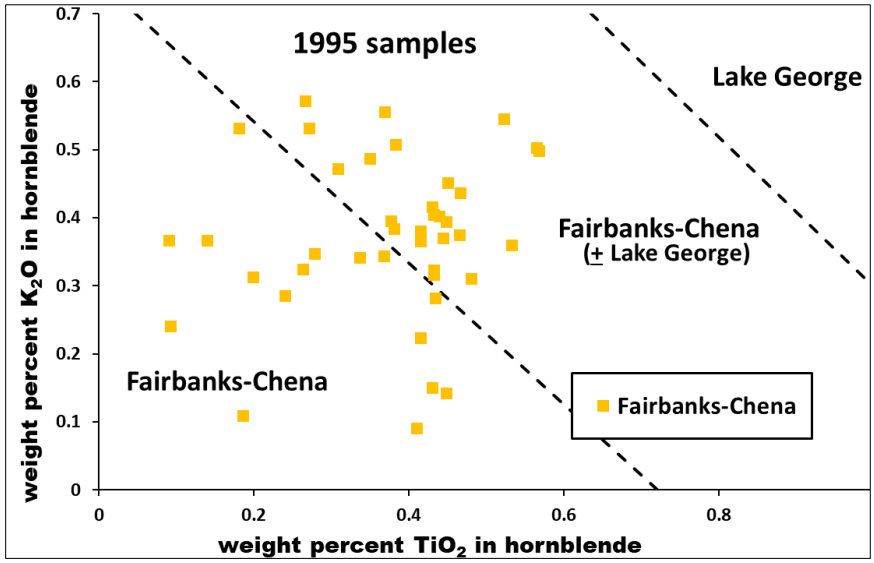

Figure 17. Weight percent TiO_2 versus K_2O in hornblende for Fairbanks area amphiboles analyzed in 1996 and 2025. Dashed black lines are empirical and separate Lake George from Fairbanks-Chena samples.

Plagioclase from Fairbanks-area amphibolite is probably the most straightforward of the various plagioclase composition sets (figs. 6, 9, 12, and 15). All analyses yield less than 36 percent anorthite component (fig. 18), and albite is rare (or perhaps analyses of such were rare). Most samples yielded a range of compositions, generally $An_{18–35}$. These samples unquestionably fall into the Fairbanks-Chena category.

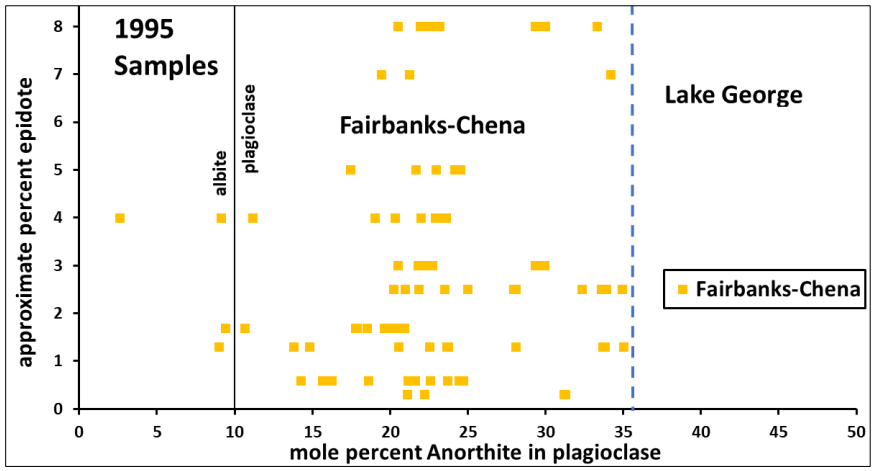

Figure 18. Mole percent anorthite versus percent epidote for Fairbanks area amphibolite samples analyzed in 1996 and 2025.

DISCUSSION

The objective of this study was to determine whether mineral compositions from metamafic rocks (primarily amphibolite) could be employed to distinguish among different Interior Alaskan assemblages (as defined by Dusel-Bacon and others, 2006). To test this hypothesis, we analyzed both amphibole and plagioclase, as these minerals exhibit considerable compositional variation and are ubiquitous in metamafic rocks. Each mineral has some associated caveats, discussed below.

Amphiboles are compositionally much more complex than plagioclases, and cation distribution requires making choices about Fe^{2+} versus Fe^{3+}. We have followed the recommendations of Leake and others (1997) and follow the procedures described in Rock and Leake (1984). Such calculations require relatively high-quality analyses. Our work shows that clean compositional separation between Lake George and Fairbanks-Chena amphiboles can be accomplished with WDS-EPMA analyses (figs. 13, 14, 16, and 17); compositional separation between Lake George and Fortymile River or Fairbanks-Chena by using less-accurate standard-modified EDS techniques is more ambiguous, but seemingly sufficient (figs. 4, 5, 7, 8, 10, and 11). Fortymile River and Fairbanks-Chena amphiboles have generally indistinguishable compositions, presumably because both experienced mostly epidote-amphibolite conditions. Both plot above and below Lake George amphiboles on EDS-based atomic Si versus Na + K (A site) plots (figs. 4, 7, and 10). Approximately half of Fortymile River amphiboles and 5–10 percent of Fairbanks-Chena samples plot above Lake George amphiboles. Future WDS analyses of Fortymile River amphiboles could help better constrain this difference.

In terms of EDS-based TiO_2 versus K_2O content (figs. 5, 8, and 11), three regions are identified: (a) exclusively Lake George (highest TiO_2–K_2O), (b) some of all assemblages (intermediate TiO_2–K_2O), and (c) not Lake George (lowest TiO_2–K_2O). In contrast, the diagrams based on WDS analyses show no compositional overlap between Lake George and Fairbanks-Chena amphiboles (figs. 14 and 17). We propose this is because WDS is more accurate than standard-modified EDS at identifying the relatively low concentrations of these elements.

The discrimination based on TiO_2–K_2O is not a bulk composition effect as the elemental abundances of all major elements in Lake George, Fairbanks-Chena, and Fortymile River assemblage amphibolites are essentially indistinguishable (fig. 2). Regarding TiO_2, every amphibolite sample contains at least two percent rutile + ilmenite + titanite, confirming that there is plenty of Ti present in the rocks. Metamorphic conditions (higher grade) in Lake George amphibolite presumably favored the incorporation of Ti into the hornblende. Zakrutkin and Grigorenko (1967) report an increase in Ti with increasing metamorphic grade for common metamorphic amphiboles.

We do not know the explanation for the apparently higher K_2O content of Lake George amphiboles relative to amphiboles from the other assemblages (for example, fig. 14). This is true despite the higher Na + K (A site) observed in Fortymile River relative to Lake George amphiboles (figs. 8 and 16). We note that in our amphiboles, the atomic Na/K ratio is commonly 3:1–10:1 (see accompanying digital data), and that the B site typically contains 1.6–1.9 Ca per formula unit (out of 2.0). Since Na_B (2-Ca per formula unit) fills the B site and there is much more Na than K, a small increase in K_2O does not necessarily translate to an increase in $(Na + K)_A$. Also note that Fairbanks-Chena amphiboles typically contain less $(Na + K)_A$ than Lake George amphiboles as well as less K_2O (figs. 13 and 14, respectively).

Plagioclase should be more straightforward, and the results are much easier to visualize, but there are analytical, alteration, and/or recrystallization issues. Analytically, even with a defocused beam and relatively low current, Na is ejected from plagioclase (especially high-Na plagioclase) due to the high-energy electron beam. Consequently, we set the standard-modified EDS analysis time for plagioclase lower than for other minerals. This potentially causes accuracy problems; however, the comparison of average plagioclase composition by the two methods (fig. 3) shows excellent agreement. (We rejected a modest proportion, 10–20 percent, of the high-Na feldspar analyses as having unrealistic compositions.) In principle, WDS analyses can encounter similar problems, but our repeated analysis of a relatively high-Na plagioclase standard yielded reproducible, appropriate results.

More problematic is the apparently more common (than amphibole) recrystallization of plagioclase during higher temperature regional metamorphism, low-pressure contact metamorphism, or retrograde metamorphism. Intuitively, one would expect that the presence of a high-Ca phase like epidote would restrict the amount of Ca available for plagioclase; thus, epidote-absent rocks could contain higher Ca-plagioclase than epidote-bearing rocks. This is seen, for example, in the map area just northwest of Chicken (figs. 1 and A1), where, progressing north, one moves from epidote amphibolites with $An_{15–35}$ plagioclase to (garnet) amphibolite with $An_{20–45}$ plagioclase (21RN568, fig. 6). This sample, however, has amphiboles with Fortymile River type composition (figs. 4 and 5). Somewhat similarly, sample 24RN391 is located close to the Chena Hot Springs batholith (fig. A13), and it contains relict $An_{20–35}$ plagioclase surrounded by younger $An_{70–85}$ plagioclase (fig. 15). Sample 24JWB158 is located even closer to a granite body (fig. A11),

and it contains (altered relict?) $An_{55–60}$ plagioclase and younger $An_{85–90}$ plagioclase. In these cases, destruction of regional metamorphic epidote during contact metamorphism causes the plagioclase in such rocks to acquire Lake George-like compositions. Amphiboles are resistant to such changes because the upper stability limit of epidote (approximately 570–650 °C, depending on iron content, pressure, and oxidation state; Liou, 1973) is much lower than that of hornblende.

If fluids permeate rocks during cooling from high temperatures, the opposite happens: higher-Ca plagioclase is converted to lower-Ca plagioclase (ultimately to albite) + epidote–clinozoisite. In such cases, some of the hornblende is also converted to actinolite, but generally less so than the plagioclase. For example, the feldspar in sample 21ET167 is exclusively albite ($An_{0–3}$; pale green triangles in fig. 6) whereas half of the amphibole is actinolite and half hornblende (pale green triangles in fig. 4). Sample 21RN240, from the same general area (fig. A5) yielded plagioclase with a wide range of compositions ($An_{3–40}$; darker green triangles in fig. 6) and contained mostly hornblende with minor actinolite (darker green triangles in fig. 4). We interpret these two samples from the McComb Plateau in the Alaska Range as partly retrograded Lake George assemblage, despite the paucity of higher-Ca plagioclase, because the amphibole compositions plot with Lake George samples (figs. 4 and 5). In cases like these, Lake George samples possess non-Lake George (less than An_{35}) plagioclase.

In sum, in geologically simple cases, both plagioclase and amphiboles yield compositions that appear to identify amphibolites of the Lake George Assemblage versus those of either Fortymile River or Fairbanks-Chena Assemblages. In particular, plagioclase with more than 41 percent anorthite component is mostly diagnostic for the Lake George Assemblage. Especially where contact or retrograde metamorphism is extensive, however, plagioclase compositions are less reliable than those of amphiboles. In most cases, standard-modified EDS analyses are adequate for such discrimination; however, WDS is clearly preferable. A useful strategy would be to start with EDS to ensure the appropriate minerals are present, and then follow up with WDS.

By-and-large, the assignments based on mineral compositions are in agreement with the scheme presented by Dusel-Bacon and others (2006). Complications in Fortymile River versus Lake George assignments are primarily in regions of previously unrecognized steeply dipping faults that displace the inferred low-angle fault between the two or better indicate the location of the low-angle fault (figs. A2-A7). Similarly, much of the area south of the greenschist facies belt (assigned to Lake George Assemblage) yielded amphibolites with ‘Lake George-type’ compositions. All amphibolites from north of the greenstone belt, assigned to the Fairbanks-Chena assemblage, yielded amphiboles with compositions that contrasted with Lake George amphibole compositions, and plagioclase mostly containing less than 41 percent anorthite component. However, several cases of clearly Fairbanks-Chena compositions occurring south of the greenschist belt are documented (figs. A10, A12, A14). These occurrences indicate that Fairbanks-Chena assemblage rocks are more common than previously reported by Dusel-Bacon and others (2006).

Twelker and others (2025a) first recognized this more widespread distribution of the Fairbanks-Chena Assemblage based on rock types in the Richardson Mining District that better matched Fairbanks-Chena than those in the Lake George Assemblage (Twelker and others, 2025b). Based in part on industry drill information reported in Graham (2002), Twelker and others (2025a, b) concluded that Fairbanks-Chena Assemblage rocks structurally overlie Lake George assemblage rocks. Thus, the presence of these new Fairbanks-Chena amphibolite sites has important implications with respect to previously unrecognized low-angle faults in central interior Alaska.

CONCLUSION

We show that amphibolite facies meta-mafic rocks in Interior Alaska are characterized by hornblende (in the broad sense of an aluminous calcic amphibole) + plagioclase, whereas greenschist facies meta-mafic rocks (e.g., Klondike, sample 22ET093, brown triangles in fig. 7) contain actinolite + albite. Partial overprinting by retrograde fluids can cause minor to major amounts of actinolite + albite in amphibolites, but in our experience, at least remnants of hornblende remain. Within the amphibolite and epidote-amphibolite facies rocks, compositional contrasts in amphibole and plagioclase compositions can distinguish Fortymile River and Fairbanks-Chena assemblage rocks from Lake George assemblage rocks. Fortymile River and Fairbanks-Chena assemblage rocks appear to be spatially separated from each other (Dusel-Bacon and others, 2006), so the lack of a clear distinction between these two is less important.

Based on our experience, standard-modified EDS analyses yield acceptable results for discriminating between Lake George assemblage amphiboles and other assemblages. However, the more accurate WDS analyses appear to yield cleaner separation and less ambiguity in assemblage composition. We recommend this analytical technique for future studies.

Based on our data, Fairbanks-Chena assemblage rocks are more common in interior Alaska than previously assumed, requiring the presence of previously unmapped low-angle faults. Continued use of this compositional tool may lead to the discovery of more Fairbanks-Chena assemblage rocks and associated cryptic structures in interior Alaska.

ACKNOWLEDGMENTS

The authors thank J. Wes Buchanan for his review, which improved the quality of the manuscript, and the University of Alaska Fairbanks Advanced Instrumentation Laboratory (UAF–AIL) manager, Dr. Nathan Graham, who helped set up the 2024 WDS analyses. We also thank Evan Twelker, Travis Naibert, Mike Barrera, Dave Szumigala, Alicja Wypych, Michelle Gavel, Wes Buchanan, Alec Wildland, Sean Regan, David Harvey, Izzy Muller, Serena Fessenden, Noel Blackwell, Lily Norwood, and Marisa Acosta, who mapped with the authors at various times between 2021 and 2024, procured samples used in this study, and provided helpful observations and ideas. K. Clautice, D. Solie, T. Bundtzen, G. Laird, and R. Reifenstuhl mapped with Newberry in 1995 and provided samples and discussion. Dr. Ken Severin assisted with those WDS analyses.

Much of this work was performed at the UAF-AIL, and the authors gratefully acknowledge use of the UAF-AIL electron microprobe acquired with support from the National Science

Foundation, Major Research Instrumentation Program Award Number 1126898. We profusely thank past and present personnel of UAF-AIL.

This project was jointly funded by the State of Alaska and the U.S. Geological Survey Earth Mapping Resources Initiative (Earth MRI) through cooperative agreements G20AC00156, G21AC00336, G22AC00288, G23AC00372, and G24AC00323. The views and conclusions contained in this document are those of the authors and should not be interpreted as representing the opinions or policies of the U.S. Geological Survey. Mention of trade names or commercial products does not constitute their endorsement by the U.S. Geological Survey.

REFERENCES

Buchanan, J.W., Wypych, Alicja, Barrera, M.L., Biegel, J.M., Gavel, M.M., Harvey, D.A., Ketcham, R.A., Muller, I.P., Naibert, T.J., Newberry, R.J., Regan, S.P., Szumigala, D.J., Twelker, Evan, and Wildland, A.D., 2025, Geochemical data from samples collected in 2023 for the Chena and Mount Harper projects, Big Delta, Circle, Fairbanks, and Eagle quadrangles, Alaska: Alaska Division of Geological & Geophysical Surveys Raw Data File 2024-2, 5 p. https://doi.org/10.14509/31123

Deer, W.A., Howie, R.A., and Zussman, Jack, 1997, Double-chain silicates (2nd ed.): London, The Geological Society, 764 p.

Dusel-Bacon, Cynthia, Hopkins, M.J., Mortensen, J.K., Dashevsky, S.S., Bressler, J.R., and Day, W.C., 2006, Paleozoic tectonic and metallogenic evolution of the pericratonic rocks of east-central Alaska and adjacent Yukon Territory, in Colpron, Maurice, and Nelson, J.L., eds., Paleozoic evolution and metallogeny of pericratonic terranes at the ancient Pacific margin of North America, Canadian and Alaskan Cordillera: Geological Association of Canada Special Paper 45, p. 25–74.

Gavel, M.M., Wypych, Alicja, Naibert, T.J., Twelker, Evan, Newberry, R.J., Barrera, M.L., Szumigala, D.J., Truskowski, C.M., Muller, I.P., Fessenden, S.N., Blackwell, N.J., Harvey, D.A., and Wildland, A.D., 2025, Bedrock geologic map of the Mount Harper–Middle Fork area, Eagle Quadrangle, Alaska: Alaska Division of Geological & Geophysical Surveys Preliminary Interpretive Report 2025-2D, 1 sheet, scale 1:100,000. https://doi.org/10.14509/31652

Graham, G.E., 2002, Geology and gold mineralization of the Richardson district, east-central Alaska: unpublished M.S. thesis, University of Alaska Fairbanks, 150 p.

Joy, B.R., Keskinen, M.J., and Newberry, R.J., 1996, Preliminary thermobarometry and microprobe mineral compositions, Fairbanks area schists and amphibolites: Alaska Division of Geological & Geophysical Surveys Public Data File 96-12, 15 p. https://doi.org/10.14509/1736

Leake, B.E., Woolley, A.R., Arps, C.E.S., Birch, W.D., Gilbert, M.C., and others, 1997, Nomenclature of amphiboles: Report of the subcommittee on amphiboles of the

International Mineralogical Association, Commission on New Minerals and Mineral Names: American Mineralogist, v. 82, p. 1019–1037.

Liou, J.G., 1973, Synthesis and stability relations of epidote, $Ca_2Al_2FeSi_3O_{12}(OH)$: Journal of Petrology, v. 14, p. 381–413.

Moshrefzadeh, J.A., and Newberry, R.J., 2025, Electron probe microanalyzer data collected on samples from the Chena and Steese projects, Yukon–Tanana Uplands, Alaska: Alaska Division of Geological & Geophysical Surveys Raw Data File 2025-13, 6 p. https://doi.org/10.14509/31537

Naibert, T.J., Wypych, Alicja, Newberry, R.J., Twelker, Evan, Gavel, M.M., Wildland, A.D., Barrera, M.L., Avirett, D.F., Muller, I.P., Blackwell, N.J., and Szumigala, D.J., 2024, Bedrock geologic map of the Taylor Mountain area, Eagle and Tanacross quadrangles, Alaska, in Naibert, T.J., ed., Geologic investigation of the Western Tanacross and Taylor Mountain areas, Tanacross and Eagle quadrangles, Alaska: Alaska Division of Geological & Geophysical Surveys Preliminary Interpretive Report 2024-6B, 1 sheet, scale 1:100,000. https://doi.org/10.14509/31168

Naibert, T.J., Newberry, R.J., Twelker, Evan, Wypych, Alicja, Gavel, M.M., Barrera, M.L., Szumigala, D.J., Truskowski, C.M., Muller, I.P., Fessenden, S.N., Buchanan, J.W., Blackwell, N.J., Harvey, D.A., and Wildland, A.D., 2025, Bedrock geologic map of the Volkmar River–Healy River area, Big Delta and Mount Hayes quadrangles, Alaska: Alaska Division of Geological & Geophysical Surveys Preliminary Interpretive Report 2025-2C, 1 sheet, scale 1:100,000. https://doi.org/10.14509/31651

Newberry, R.J., Bundtzen, T.K., Clautice, K.H., Combellick, R.A., Douglas, Tom, Laird, G.M., Liss, S.A., Pinney, D.S., Reifenstuhl, R.R., and Solie, D.N., 1996, Preliminary geologic map of the Fairbanks mining district, Alaska: Alaska Division of Geological & Geophysical Surveys Public Data File 96-16, 17 p., 2 sheets, scale 1:63,360. https://doi.org/10.14509/1740

Newberry, R.J., and Twelker, Evan, 2021, Metamorphism of the Ladue River–Mount Fairplay area, in Twelker, Evan, ed., Geologic investigation of the Ladue River–Mount Fairplay area, eastern Alaska: Alaska Division of Geological & Geophysical Surveys Report of Investigation 2021-5B, p. 33–39. https://doi.org/10.14509/30736

Newberry, R.J., Twelker, Evan, Naibert, T.J., Wypych, Alicja, Gavel, M.M., Barrera, M.L., Szumigala, D.J., Truskowski, C.M., Muller, I.P., Fessenden, S.N., Buchanan, J.W., Blackwell, N.J., Harvey, D.A., and Wildland, A.D., 2025, Bedrock geologic map of the Goodpaster River–Shaw Creek area, Big Delta Quadrangle, Alaska: Alaska Division of Geological & Geophysical Surveys Preliminary Interpretive Report 2025-2B, 1 sheet, scale 1:100,000. https://doi.org/10.14509/31650

Nokleberg, W.J., Aleinikoff, J.N., Lange, I.M., Silva, S.R., Miyaoka, R.T., Schwab, C.E., and Zehner, R.E., 1992, Preliminary geologic map of the Mount Hayes Quadrangle, eastern

Alaska Range, Alaska: U.S. Geological Survey Open-File Report 92-594, 39 p., 1 sheet, scale 1:250,000.

Robinson, M.S., Smith, T.E., and Metz, P.A., 1990, Bedrock geology of the Fairbanks mining district: Alaska Division of Geological & Geophysical Surveys Professional Report 106, 2 sheets, scale 1:63,360. https://doi.org/10.14509/2287

Rock, N.M.S., and Leake, B.E., 1984, The International Mineralogical Association amphibole nomenclature scheme: computerization and its consequences: Mineralogical Magazine, v. 48, p. 211–227.

Twelker, Evan, Newberry, R.J., Wypych, Alicja, Naibert, T.J., Wildland, A.D., Sicard, K.R., Regan, S.P., Athey, J.E., Wyatt, W.C., and Lopez, J.A., 2021, Bedrock geologic map of the Ladue River–Mount Fairplay area, Tanacross and Nabesna quadrangles, Alaska, in Twelker, Evan, ed., Geologic investigation of the Ladue River–Mount Fairplay area, eastern Alaska: Alaska Division of Geological & Geophysical Surveys Report of Investigation 2021-5A, p. 1–32, 1 sheet, scale 1:100,000. https://doi.org/10.14509/30735

Twelker, Evan, Newberry, R.J., Naibert, T.J., and Wypych, Alicja, 2025a, Bedrock geologic map of the Richardson Mining District, Alaska: Alaska Division of Geological & Geophysical Surveys Preliminary Interpretive Report 2025-2A, 1 sheet, scale 1:100,000. https://doi.org/10.14509/31649

Twelker, Evan, Newberry, R.J., Naibert, T.J., Wypych, Alicja, Gavel, M.M., Barrera, M.L., Szumigala, D.J., Truskowski, C.M., Muller, I.P., Fessenden, S.N., Blackwell, N.J., Harvey, D.A., and Wildland, A.D., 2025b, Bedrock geologic maps of the Mount Harper–Middle Fork area, Volkmar River–Healy River area, Goodpaster River–Shaw Creek area, and the Richardson Mining District, Alaska: Alaska Division of Geological & Geophysical Surveys Preliminary Interpretive Report 2025-2, 38 p. https://doi.org/10.14509/31648

Wilson, F.H., Hults, C.P., Mull, C.G., and Karl, S.M., 2015, Geologic map of Alaska: U.S. Geological Survey Scientific Investigations Map 3340, 196 p., 2 sheets, scale 1:1,584,000.

Wypych, Alicja, Naibert, T.J., Athey, J.E., Newberry, R.J., Sicard, K.R., Twelker, Evan, Werdon, M.B., Willingham, A.L., and Wyatt, W.C., 2018, Major-oxide and trace-element geochemical data from rocks collected in 2018 for the Northeast Tanacross project, Tanacross C-1, C-2, D-1, and D-2 quadrangles, Alaska: Alaska Division of Geological & Geophysical Surveys Raw Data File 2018-4, 4 p. https://doi.org/10.14509/30113

Wypych, Alicja, Gavel, M.M., Naibert, T.J., Avirett, D.F., Barrera, M.L., Hubbard, A.K., Newberry, R.J., Regan, S.P., Twelker, Evan, Wildland, A.D., and Wyatt, W.C., 2022a, Geochemical data from samples collected in 2021 for the Taylor Mountain project, Tanacross and Eagle quadrangles, Alaska: Alaska Division of Geological & Geophysical Surveys Raw Data File 2022-4, 3 p. https://doi.org/10.14509/30843

Wypych, Alicja, Gavel, M.M., Naibert, T.J., Avirett, D.F., Barrera, M.L., Hubbard, A.K.,

Newberry, R.J., Regan, S.P., Twelker, Evan, Wildland, A.D., and Wyatt, W.C., 2022b, Geochemical data from samples collected in 2020 and 2021 for the Western Tanacross project, Tanacross Quadrangle, Alaska: Alaska Division of Geological & Geophysical Surveys Raw Data File 2022-5, 3 p. https://doi.org/10.14509/30844

Wypych, Alicja, Twelker, Evan, Naibert, T.J., Gavel, M.M., Newberry, R.J., Szumigala, D.J., Wildland, A.D., Barrera, M.L., Harvey, D.A., Muller, I.P., Fessenden, S.N., and Blackwell, N.J., 2023, Geochemical data from samples collected in 2022 for the Mount Harper geologic mapping project, Big Delta, Mount Hayes, and Eagle quadrangles, Alaska: Alaska Division of Geological & Geophysical Surveys Raw Data File 2023-24, 3 p. https://doi.org/10.14509/31089

Wypych, Alicja, Naibert, T.J., Newberry, R.J., Twelker, Evan, Gavel, M.M., Wildland, A.D., Szumigala, D.J., Regan, S.P., Avirett, D.F., Barrera, M.L., Bernard, C.M., Blackwell, N.J., Fessenden, S.N., Harvey, D.A., Hubbard, A.K., Masterman, S.S., Muller, I.P., Turner, M.M., and Wyatt, W.C., 2024, Bedrock geologic map of the Western Tanacross area, Tanacross Quadrangle, Alaska, in Naibert, T.J., ed., Geologic investigation of the Western Tanacross and Taylor Mountain areas, Tanacross and Eagle quadrangles, Alaska: Alaska Division of Geological & Geophysical Surveys Preliminary Interpretive Report 2024-6C, 1 sheet, scale 1:100,000. https://doi.org/10.14509/31169

Zakrutkin, V.V., and Grigorenko, M.V., 1968, Titanium and alkalies in amphiboles in metamorphism: Transactions (Doklady) of the USSR Academy of Sciences, Earth Science Section, v. 173, p. 197–198.

APPENDIX A: DETAILED LOCATION AND GEOLOGIC MAPS
2021 Geologic Investigations

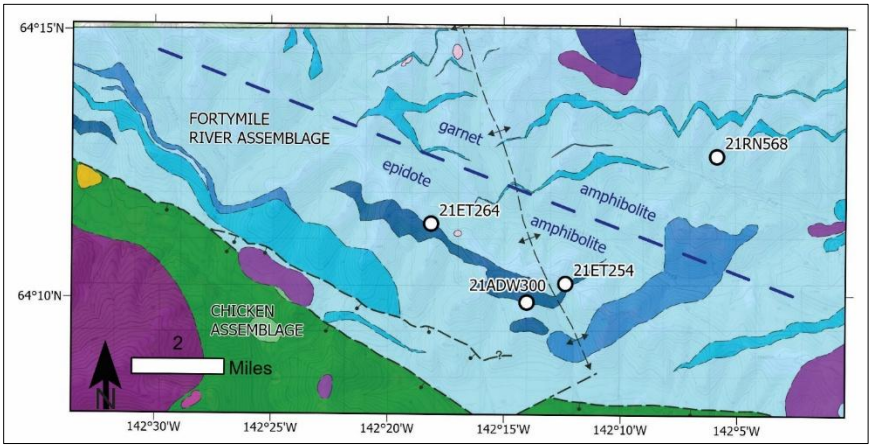

Figure A1. Northeast corner of the Taylor Mountain geologic map (modified from Naibert and others, 2024) showing amphibolite sample locations and approximate location of boundary between epidote amphibolite and amphibolite facies in the Fortymile River assemblage (blue dashed line).

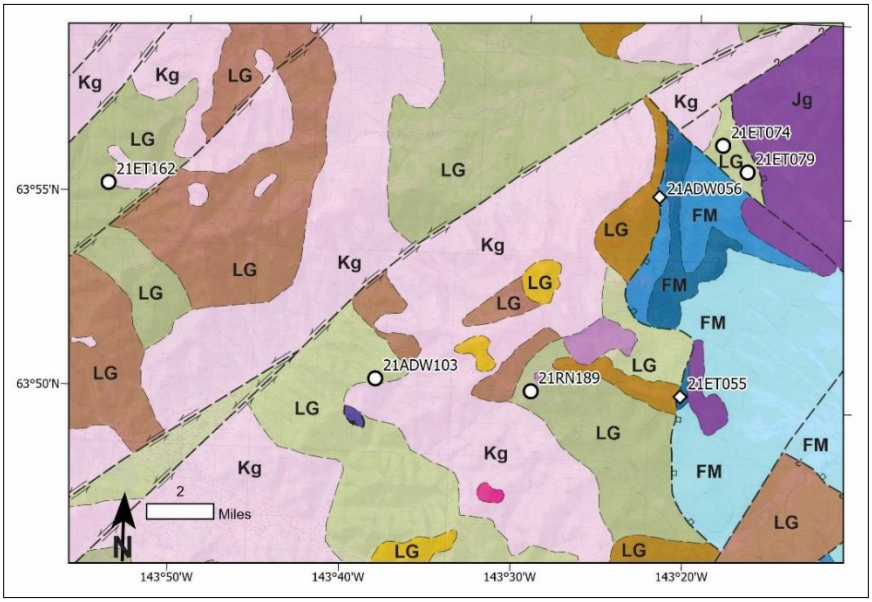

Figure A2. Northwest corner of the Northwest Tanacross geologic map (modified from Wypych and others, 2024) showing amphibolite sample locations. White diamond = Fortymile River sample; white circle = Lake George sample. Kg = Cretaceous granitic; Jg = Jurassic granitic; LG = Lake George (shades of brown/tan); FM = Fortymile River (shades of blue).

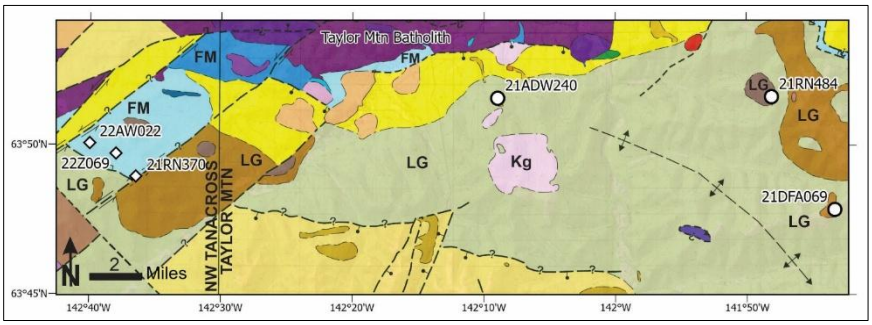

Figure A3: South edge of the Taylor Mountain and adjacent NW Tanacross geologic maps (modified from Naibert and others, 2024, and Wypych and others, 2024) showing amphibolite sample locations. Diamond = Fortymile River sample, circle = Lake George sample. Map abbreviations: Kg = Cretaceous granitic, LG = Lake George (shades of brown/tan), FM = Fortymile River (shades of blue). Note two 2022 samples on the western end of the map.

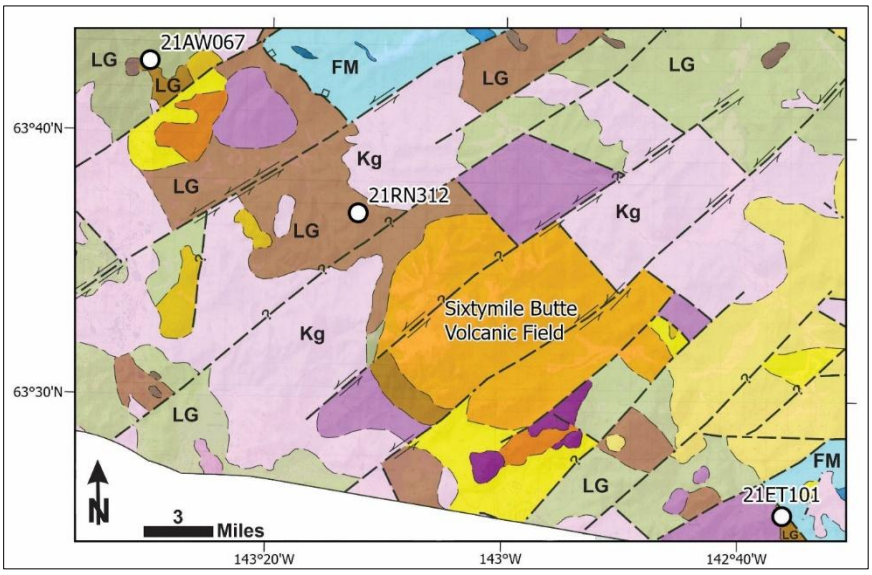

Figure A4. Southeast corner of the Northwest Tanacross geologic map (modified from Wypych and others [2024]) showing Lake George amphibolite sample locations. Kg = Cretaceous granitic; LG = Lake George; FM = Fortymile River.

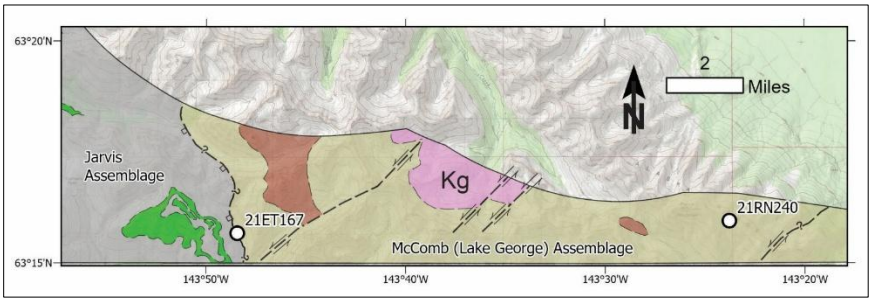

Figure A5. Alaska Range sliver of the Northwest Tanacross geologic map (modified from Wypych and others [2024]) showing McComb (Lake George) amphibolite sample locations.

2022 Geologic Investigations

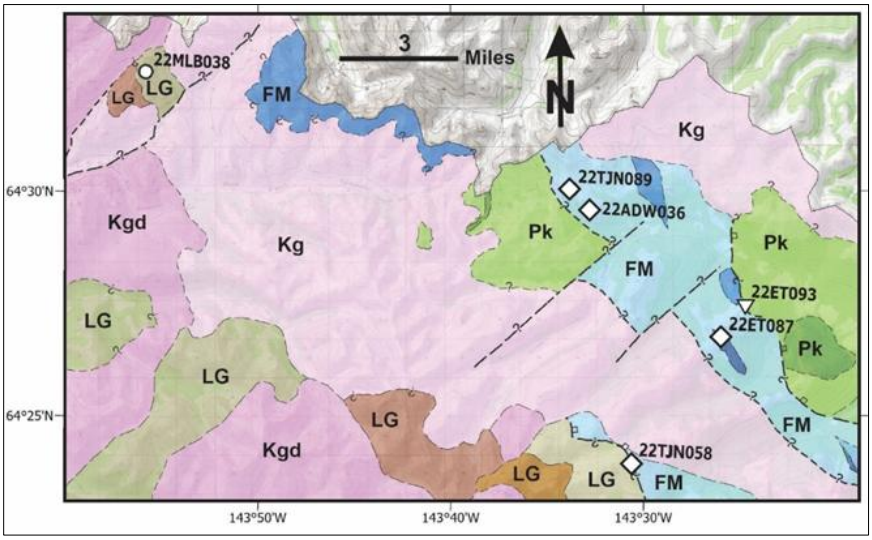

Figure A6. Northern edge of the Mount Harper–Middle Fork geologic map area (modified from Gavel and others, 2025) showing meta-mafic rock sample locations. White triangle = Klondike; white diamond = Fortymile River; white circle = Lake George. Map abbreviations: Kg = Cretaceous granite; Kgd = Cretaceous granodiorite; LG = Lake George; FM = Fortymile River; Pk = Klondike.

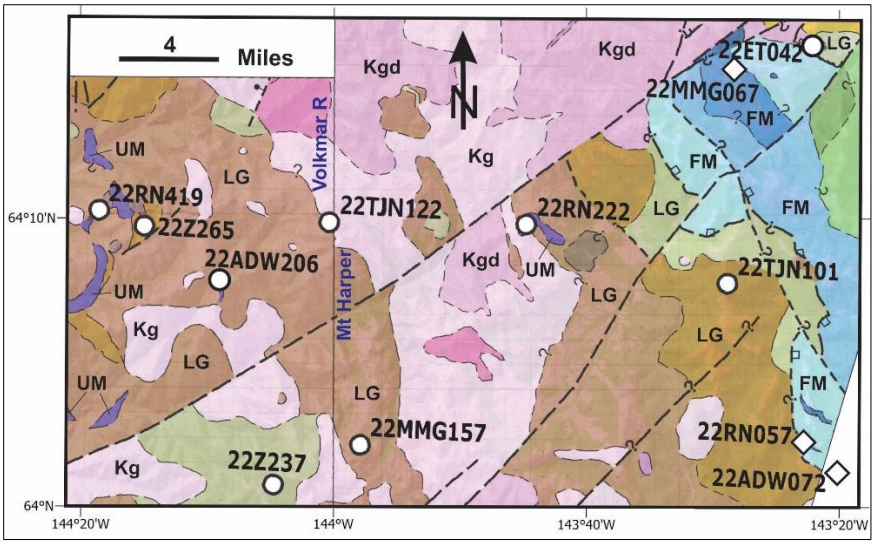

Figure A7. Southern Mount Harper–Middle Fork geologic map area and adjacent Volkmar River area (modified from Gavel and others, 2025, and Naibert and others, 2025) showing amphibolite sample locations. White diamonds = Fortymile River, white circles = Lake George. Map abbreviations: Kg = Cretaceous granite; Kgd = Cretaceous granodiorite; LG = Lake George; FM = Fortymile River; UM = meta-ultramafic rocks.

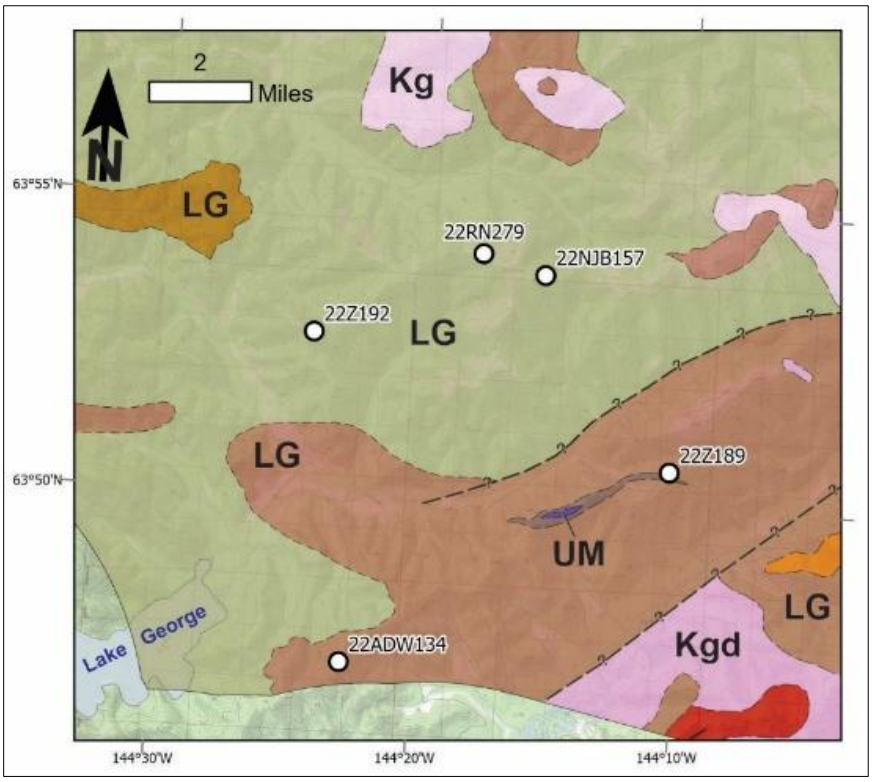

Figure A8. Geologic map of the southeast Volkmar River area (modified from Naibert and others, 2025) showing Lake George amphibolite sample locations. Map abbreviations: Kg = Cretaceous granite; Kgd = Cretaceous granodiorite; LG = Lake George; UM = meta-ultramafic rocks. Note Lake George at the southwest corner.

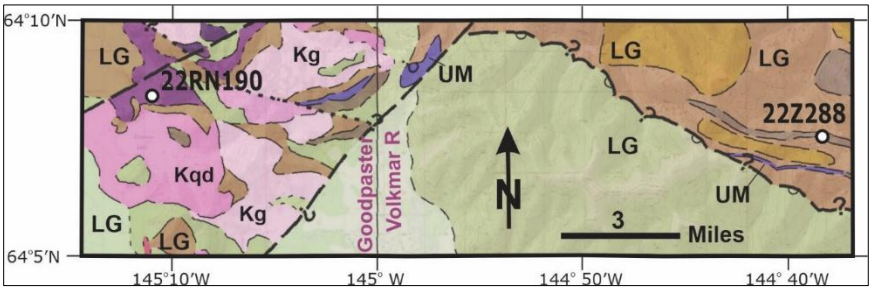

Figure A9. Geologic map of the western Volkmar River area and adjacent Goodpasture River area (modified from Naibert and others [2025] and Newberry and others [2025]) showing Lake George amphibolite sample locations. Kg = Cretaceous granite; Kqd = Cretaceous quartz diorite; LG = Lake George; UM = meta-ultramafic rocks.

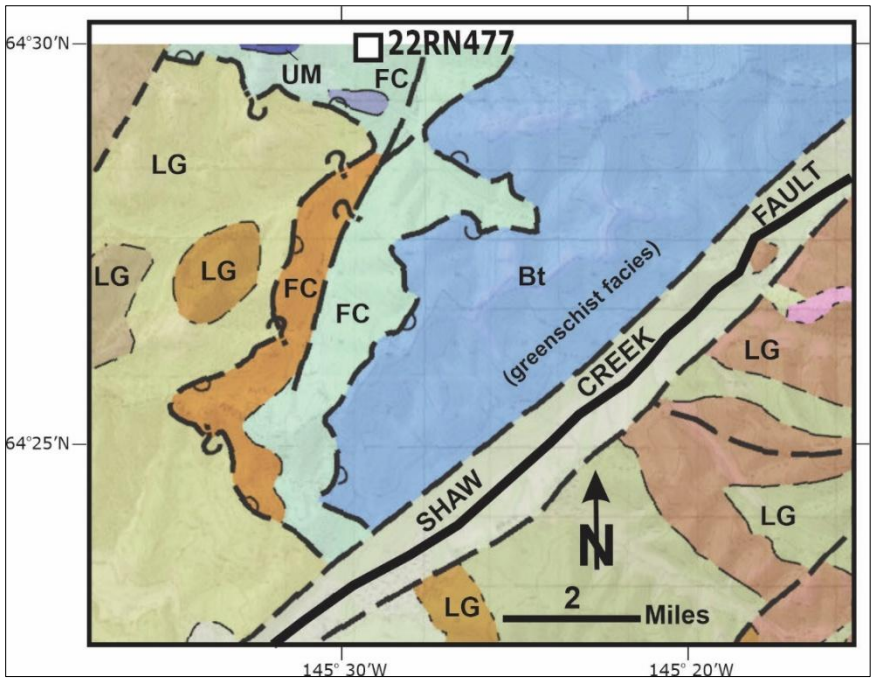

Figure A10. Geologic map of the northeast Richardson mining district and adjacent Goodpasture River area (modified from Twelker and others, 2025, and Newberry and others, 2025) showing a Fairbanks-Chena amphibolite sample location (white square). LG = Lake George unit; FC = Fairbanks-Chena unit; UM = meta-ultramafic rocks; Bt = Butte unit (greenschist facies).

2023-2024 Geologic Investigations

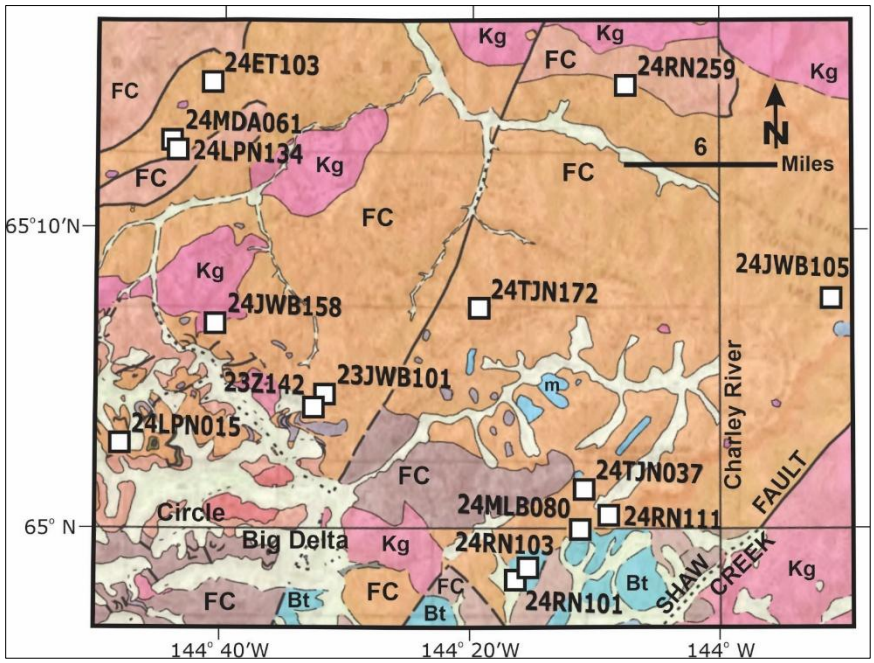

Figure A11. Geologic map of the southeast corner of the Circle Quadrangle with adjacent Charley River and Big Delta quadrangles (modified from Wilson and others [2015]) showing locations of Fairbanks-Chena amphibolite samples. Map abbreviations: FC = Fairbanks-Chena (including m = marble); Bt = Butte assemblage; Kg = Cretaceous granite.

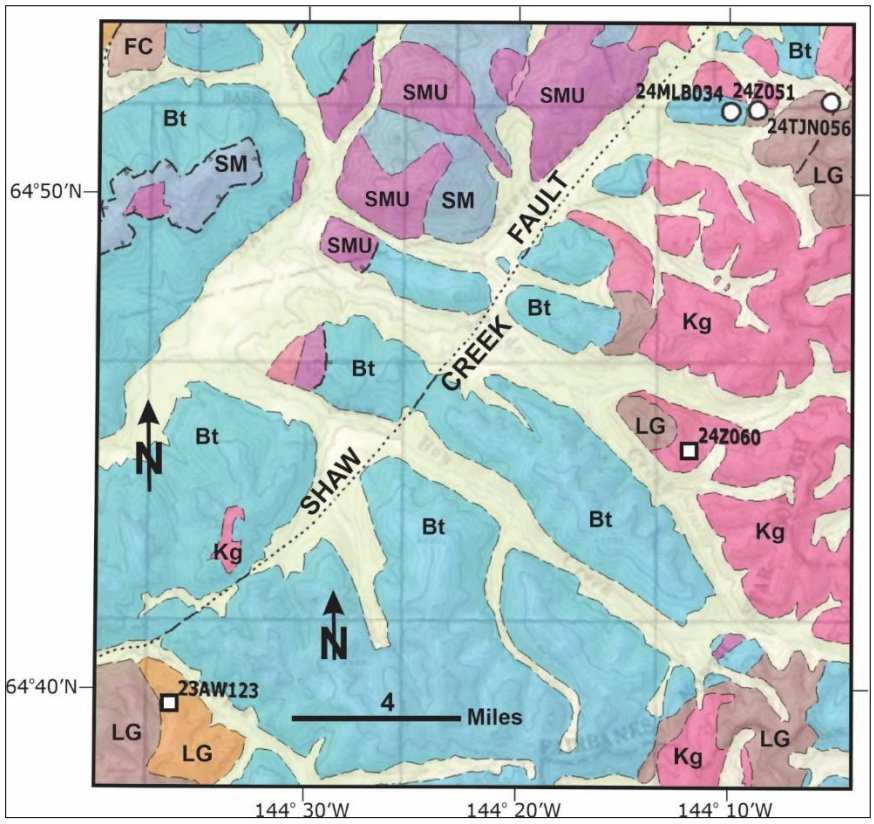

Figure A12. Geologic map of the northeast corner of the Big Delta Quadrangle (after Wilson and others [2015], with unit assignments from Dusel-Bason and others [2006]), showing location of amphibolite samples. White squares = Fairbanks-Chena; white circles = Lake George. Map abbreviations: LG = Lake George; FC = Fairbanks-Chena; Bt = Butte; SM = Seventymile terrane; SMU = Seventymile ultramafic; Kg = Cretaceous granite.

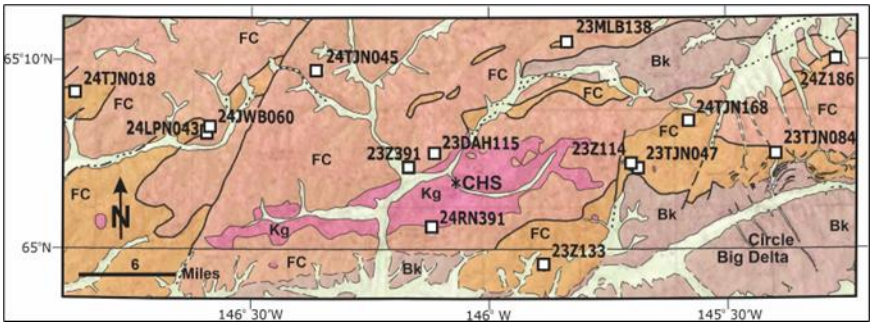

Figure A13. Geologic map of the Chena Hot Springs (CHS) area (after Wilson and others [2015], with unit assignments from Dusel-Bacon and others [2006]) showing location of Fairbanks-Chena amphibolite samples. Map abbreviations: FC = Fairbanks-Chena; Bk= Blackshell (greenschist facies); Kg = Cretaceous granite.

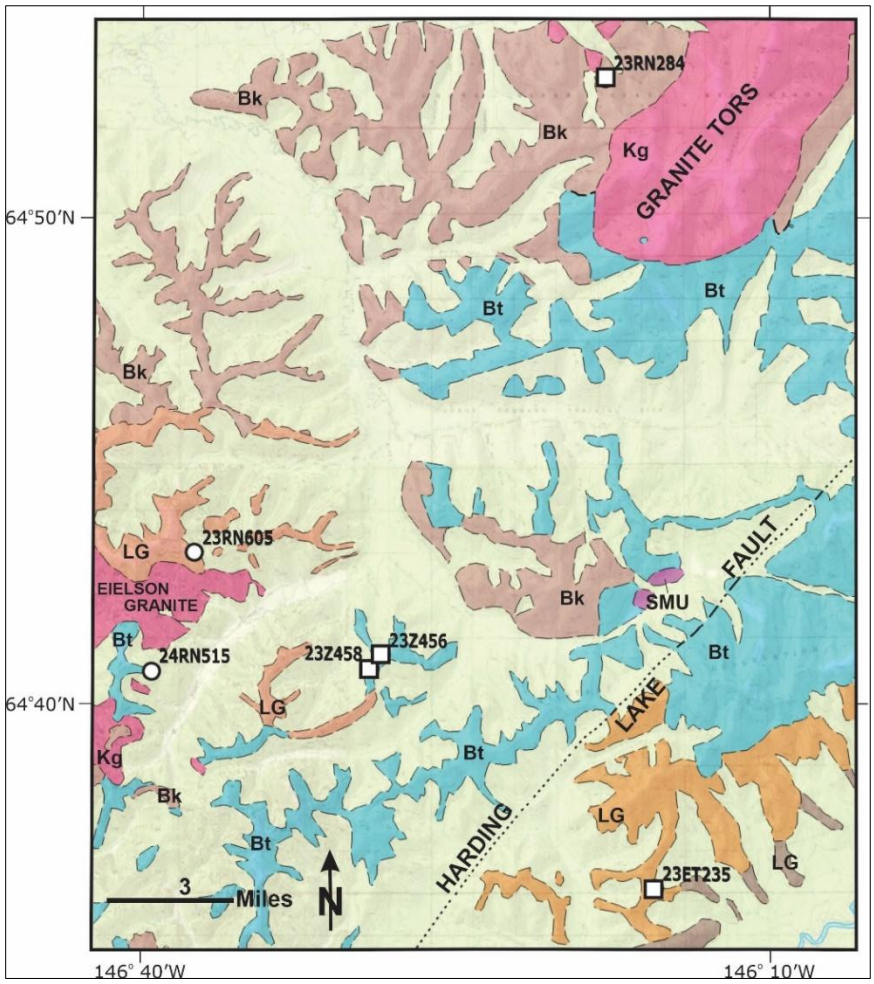

Figure A14. Geologic map of the Eielson-Granite Tors area (after Wilson and others, 2015, with unit assignments from Dusel-Bacon and others, 2006) showing location of Lake George (white circles) and Fairbanks-Chena (white squares) amphibolite samples. LG = Lake George; Bt = Butte; Bk = Blackshell (both greenschist facies); SMU = Seventymile ultramafic; Kg = Cretaceous granite. Note that several amphibolite samples are taken from areas previously mapped as greenschist facies.

1995 Geologic Investigations

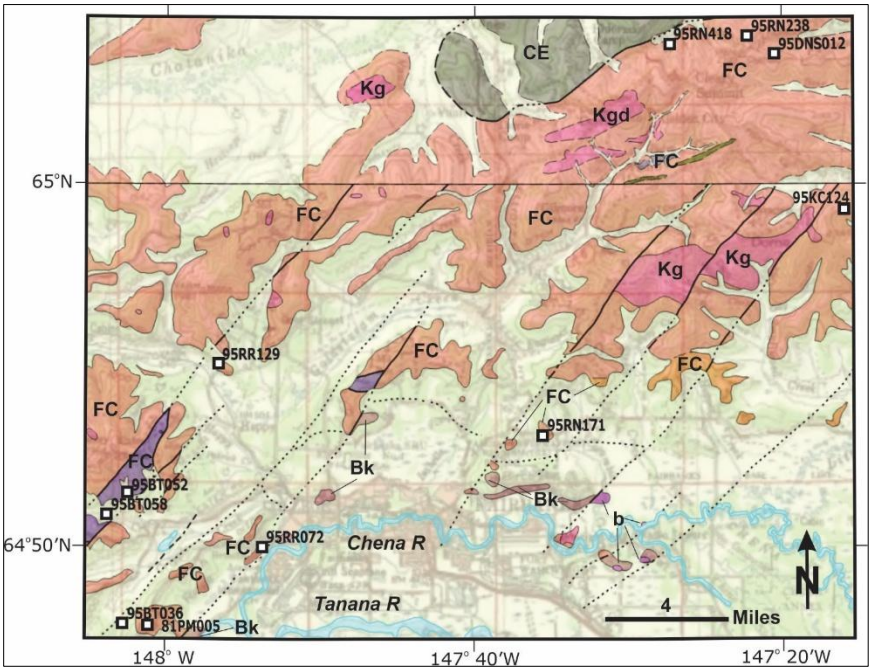

Figure A15. Geologic map of the Fairbanks area (after Wilson and others, 2015), with unit assignments from Dusel-Bacon and others (2006) showing locations of Fairbanks-Chena amphibolite samples. Map abbreviations: FC= Fairbanks-Chena; Bk = Blackshell (greenschist facies); CE = Chatanika Eclogite; Kg = Cretaceous granite; Kgd = Cretaceous granodiorite; b = Paleogene basalt.